



Efficient Variable Time-stepping Adaptive DLN Algorithms for the Allen-Cahn Equation

Yiming Chen¹ · Dianlun Luo² · Wenlong Pei¹  · Yulong Xing¹

Received: 24 September 2024 / Revised: 7 June 2025 / Accepted: 23 June 2025
© The Author(s) 2025

Abstract

We consider a family of variable time-stepping Dahlquist-Liniger-Nevanlinna (DLN) schemes, which is unconditionally non-linear stable and second order accurate, for the Allen-Cahn equation. The finite element methods are used for the spatial discretization. For the non-linear term, we combine the DLN scheme with two efficient temporal algorithms: partially implicit modified algorithm and scalar auxiliary variable algorithm. For both approaches, we prove the unconditional, long-term stability of the model energy under any arbitrary time step sequence. Moreover, we provide rigorous error analysis for the partially implicit modified algorithm with variable time-stepping. Efficient time-adaptive algorithms based on these schemes are also proposed. Several one- and two-dimensional numerical tests are presented to verify the properties of the proposed time-adaptive DLN methods.

Keywords Allen-Cahn equation · DLN method · G -stability · Time adaptivity · Finite element method · Error estimate

Mathematics Subject Classification 65M12 · 65M15 · 35K35 · 35K55

1 Introduction

The Allen-Cahn equation was first introduced by Allen and Cahn in [2] to describe the motion of anti-phase boundaries in crystalline solids. Given the domain $\Omega \subset \mathbb{R}^d$ ($d = 1, 2, 3$), $u(x, t)$ models the difference between the concentrations of two mixtures' components at

✉ Wenlong Pei
pei.176@osu.edu
Yiming Chen
chen.11042@osu.edu
Dianlun Luo
dl3572@columbia.edu
Yulong Xing
xing.205@osu.edu

¹ Department of Mathematics, The Ohio State University, Columbus, OH 43210, USA

² Department of Mathematics, Columbia University, New York, NY 10027, USA

time t , and is governed by

$$\begin{cases} u_t - \epsilon^2 \Delta u + \frac{d}{du} F(u) = 0, & x \in \Omega, 0 < t \leq T, \\ \frac{\partial u}{\partial \bar{n}} = 0, & \text{on } \partial \Omega, \end{cases} \quad (1)$$

where ϵ is the interfacial parameter. The Helmholtz free-energy density $F(u)$ and its derivative takes the form

$$F(u) = \frac{1}{4}(u^2 - 1)^2, \quad f(u) = \frac{d}{du} F(u) = u^3 - u.$$

The model energy of the Allen-Cahn equation (1) is

$$\mathcal{E}(u) := \int_{\Omega} \left(\frac{\epsilon^2}{2} |\nabla u|^2 + F(u) \right) dx,$$

which satisfies the following energy dissipation law:

$$\frac{d}{dt} \mathcal{E}(u(t)) = - \int_{\Omega} u_t^2 dx \leq 0. \quad (2)$$

Phase field models, including the Allen-Cahn equation, have been widely applied to complex moving interface problems in materials science and fluid dynamics. Over the past forty years, numerical simulations of phase field models have been extensively studied, leading to a wide array of spatial discretization techniques including finite element methods, alongside other approaches such as finite difference, finite volume, and Fourier-spectral methods. Various splitting techniques and stabilizers, coupled with classical time integrators, have been proposed to handle the potential functions in phase field models, resulting in numerous efficient and stable algorithms, as summarized in the recent survey paper [12].

Convex splitting technique is widely employed to ensure the discrete energy dissipation law [15, 18, 38, 43, 47]. The main idea is to split the potential function into the convex and concave parts, treated implicitly and explicitly, respectively. Linearly-implicit stabilizers are another popular way for gradient flows, leading to linear solvers at each time step and ensuring unconditional energy stability [31, 45, 49, 50]. Exponential integrators, transferring phase field equations into equivalent integral formulations, also achieve energy stability [3, 14, 25]. Additionally, Lagrange multiplier approach is an alternative way to construct stable numerical schemes [19], and two new classes of time-stepping schemes, invariant energy quadratization (IEQ) [34, 51, 52] and scalar auxiliary variable (SAV) schemes [1, 4], have been recently proposed. The variable step backward differentiation formulation (BDF2) method has been thoroughly investigated to show energy stability for the Allen-Cahn equation, under the ratio of successive time steps satisfying $\tau < (3 + \sqrt{17})/2$ [33]. Fully discrete interior penalty discontinuous Galerkin methods for phase field models were developed in [16, 17] to derive error estimates dependent on the polynomial order of the reciprocal model parameter ($1/\epsilon$) rather than the exponential order. Reduced-order finite element methods, based on the proper orthogonal decomposition method, can improve efficiency by reducing the dimension of the solution space while preserving the discrete energy dissipation law [32]. Explicit hybrid finite difference and operator splitting methods have demonstrated the ability to obtain pointwise boundedness of the numerical solutions [24].

In this paper, we consider a family of two-step time-stepping schemes proposed by Dahlquist, Liniger and Nevanlinna (hence the DLN method) which is unconditionally G -stable (non-linear stable) and second order accurate under non-uniform time grids [8–11]. To the best of our knowledge, *the DLN method is one of the few multi-step schemes possessing*

these two properties and thus provides a great potential in the simulations of differential equations. Recently the DLN method has been applied to various fluid models and its fine properties have been confirmed by some benchmark test problems [27, 35–37, 44]. Moreover, the DLN implementation can be simplified by adding a few lines of code to the commonly-used backward Euler scheme [28]. To utilize the unconditional G -stability to a large extent, some adaptive DLN algorithms have been proposed to balance the time accuracy and computational costs [29].

Given the initial value problem:

$$y'(t) = g(t, y(t)), \quad 0 \leq t \leq T, \quad y(0) = y_0, \tag{3}$$

with $y: [0, T] \rightarrow \mathbb{R}^d, g: [0, T] \times \mathbb{R}^d \rightarrow \mathbb{R}^d$ and $y_0 \in \mathbb{R}^d$, the two-step, variable time-stepping DLN method, with parameter $\theta \in [0, 1]$ and starting points y_0, y_1 , takes the form

$$\sum_{\ell=0}^2 \alpha_\ell y_{n-1+\ell} = \widehat{k}_n g \left(\sum_{\ell=0}^2 \beta_\ell^{(n)} t_{n-1+\ell}, \sum_{\ell=0}^2 \beta_\ell^{(n)} y_{n-1+\ell} \right), \quad n = 1, \dots, N - 1. \tag{DLN}$$

Here we denote $\{0 = t_0 < t_1 < \dots < t_n < \dots < t_{N-1} < t_N = T\}_{n=0}^N$ as the time grid on the interval $[0, T]$, with $k_n = t_{n+1} - t_n$ as the time step, $\widehat{k}_n = \alpha_2 k_n - \alpha_0 k_{n-1}$ as the average time step, and y_n as the discrete DLN solution approximating $y(t_n)$. The coefficients in (DLN) take the form

$$\begin{bmatrix} \alpha_2 \\ \alpha_1 \\ \alpha_0 \end{bmatrix} = \begin{bmatrix} \frac{1}{2}(\theta + 1) \\ -\theta \\ \frac{1}{2}(\theta - 1) \end{bmatrix}, \quad \begin{bmatrix} \beta_2^{(n)} \\ \beta_1^{(n)} \\ \beta_0^{(n)} \end{bmatrix} = \begin{bmatrix} \frac{1}{4} \left(1 + \frac{1-\theta^2}{(1+\varepsilon_n\theta)^2} + \varepsilon_n^2 \frac{\theta(1-\theta^2)}{(1+\varepsilon_n\theta)^2} + \theta \right) \\ \frac{1}{2} \left(1 - \frac{1-\theta^2}{(1+\varepsilon_n\theta)^2} \right) \\ \frac{1}{4} \left(1 + \frac{1-\theta^2}{(1+\varepsilon_n\theta)^2} - \varepsilon_n^2 \frac{\theta(1-\theta^2)}{(1+\varepsilon_n\theta)^2} - \theta \right) \end{bmatrix}. \tag{4}$$

The step variability $\varepsilon_n = (k_n - k_{n-1}) / (k_n + k_{n-1})$ represents the variation between two consecutive step sizes. On uniform time grids, step variability ε_n reduces to 0, and the coefficients $[\beta_2^{(n)}, \beta_1^{(n)}, \beta_0^{(n)}]$ simplify to $\frac{1}{4}[2 + \theta - \theta^2, 2\theta^2, 2 - \theta - \theta^2]$.

Various efficient ways to address the non-linear term of the Allen-Cahn model (1) in pursuit of unconditional energy stability have been designed. In the paper, we consider the implicit modified Crank-Nicolson method first, followed by the SAV method, which have been widely studied in the last decade. The implicit modified Crank-Nicolson scheme has been shown to provide unconditional energy stability in the Allen-Cahn model [7, 13, 42, 48]. The SAV scheme for gradient flows [39–41] achieves unconditional stability of the model energy by introducing an auxiliary scalar function, which eliminates the need to solve non-linear algebraic equations. In this context, we investigate the partially implicit modified DLN algorithm and the DLN-SAV algorithm, combined with the finite element spatial discretization, for robust simulations of the Allen-Cahn model (1). The main contributions of this work are to:

- Construct the variable step modified DLN and DLN-SAV finite element algorithms based on the DLN refactorization process (simplifying the DLN implementation by adding filters on the backward Euler scheme);
- Provide unconditional stability of model energy under arbitrary time grids for both modified DLN and DLN-SAV schemes;
- Present a rigorous proof that the fully discrete modified DLN algorithm is *1st order* accurate in time under *arbitrary time steps* and *2nd order* accurate in time under *uniform time grids*;

- Carry out a rigorous error estimate of the fully discrete DLN-SAV algorithm via a novel way to analyze the nonlinear term;
- Design time adaptive algorithms for both modified DLN and DLN-SAV schemes by the local truncation error (LTE) criterion: utilizing certain explicit time-stepping methods to estimate the LTE and adjusting time step size based on the estimator.

The rest of the paper is organized as follows. We provide necessary preliminaries and notations in Section 2. In Section 3, we study the partially implicit modified DLN scheme. We prove that the discrete model energy is unconditionally stable under variable time steps. Error estimate of the resulting fully discrete method is also provided. In Section 4, we propose the variable time-stepping DLN-SAV scheme. We prove that the corresponding model energy satisfies the discrete energy dissipation law. Moreover, we discuss how the DLN-SAV algorithm can be implemented by a simplified refactorization process: adding a few lines of code on the backward Euler-SAV (BE-SAV) scheme. Optimal error estimate of the proposed DLN-SAV algorithm in the H^1 norm is also carried out. In Section 5, the corresponding time adaptive algorithms (based on LTE criterion) are presented to improve computational efficiency. We estimate the LTE by the numerical solutions of the explicit AB2-like method (a revised two-step Adams-Bashforth method) with little or almost no extra computational costs. Several one- and two-dimensional numerical tests are presented in Section 6 to confirm the main conclusions of the paper. Conclusion remarks are provided in Section 7. Proofs of some lemmas in Section 2 are given in the appendices.

2 Preliminaries and Notations

We start by introducing some necessary notations. Let $H^r(\Omega)$ be the usual standard Sobolev space $W^{r,2}(\Omega)$ with the norm $\|\cdot\|_r$. When $r = 0$, this reduces to the inner product space $L^2(\Omega)$ with the L^2 norm $\|\cdot\|$ and the standard L^2 inner product (\cdot, \cdot) . $W^{r,\infty}(\Omega)$ is the function spaces containing all functions with essentially bounded weak derivatives up to order r . When $r = 0$, the space is reduced to $L^\infty(\Omega)$ space with norm $\|\cdot\|_\infty$. For spatial discretization, we denote $X_s^h \subset H^1(\Omega)$ as a standard finite element space on Ω with the highest polynomial degree s and a mesh diameter $h > 0$. Throughout the paper, C denotes a generic positive constant independent of h and time step size k_n . For any given function $u(x, t)$ on time grids $\{t_n\}_{n=0}^N$, $u_n = u_n(x)$ represents the function $u(\cdot, t_n)$ at time t_n .

For an arbitrary sequence $\{z_n\}_{n=0}^\infty$, we define

$$z_{n,\theta} = \frac{1+\theta}{2}z_n + \frac{1-\theta}{2}z_{n-1}, \quad z_{n,\alpha} = \sum_{\ell=0}^2 \alpha_\ell z_{n-1+\ell}, \quad z_{n,\beta} = \sum_{\ell=0}^2 \beta_\ell^{(n)} z_{n-1+\ell}, \quad (5)$$

$$z_{n,*} = \beta_2^{(n)} \left[\left(1 + \frac{k_n}{k_{n-1}}\right) z_n - \frac{k_n}{k_{n-1}} z_{n-1} \right] + \beta_1^{(n)} z_n + \beta_0^{(n)} z_{n-1}, \quad n \in \mathbb{N}, \quad (6)$$

with α_ℓ and $\beta_\ell^{(n)}$ defined in (4).

The following lemmas on stability and consistency of the DLN method (DLN) would play a key role in the numerical analysis.

Lemma 1 For any sequence $\{y_n\}_{n=0}^N$ in $L^2(\Omega)$ over \mathbb{R} , $n \in \{1, 2, \dots, N-1\}$ and $\theta \in [0, 1]$, we have

$$(y_{n,\alpha}, y_{n,\beta}) = \left\| \frac{y_{n+1}}{y_n} \right\|_{G(\theta)}^2 - \left\| \frac{y_n}{y_{n-1}} \right\|_{G(\theta)}^2 + \left\| \sum_{\ell=0}^2 \gamma_\ell^{(n)} y_{n-1+\ell} \right\|^2, \quad (7)$$

where the G -norm $\|\cdot\|_{G(\theta)}$ is defined by

$$\left\| \begin{matrix} u \\ v \end{matrix} \right\|_{G(\theta)}^2 := \frac{1}{4}(1 + \theta)\|u\|^2 + \frac{1}{4}(1 - \theta)\|v\|^2, \quad \forall u, v \in L^2(\Omega), \tag{8}$$

and the coefficients $\gamma_\ell^{(n)}$ are given by

$$\gamma_1^{(n)} = -\frac{\sqrt{\theta(1 - \theta^2)}}{\sqrt{2}(1 + \varepsilon_n \theta)}, \quad \gamma_2^{(n)} = -\frac{1 - \varepsilon_n}{2}\gamma_1^{(n)}, \quad \gamma_0^{(n)} = -\frac{1 + \varepsilon_n}{2}\gamma_1^{(n)}. \tag{9}$$

The derivation of (7) follows from algebraic calculation. We refer to [11, 27] for details, and omit the derivation here to save space. Following this, the variable time-stepping DLN method in (DLN) is unconditionally G -stable. (We refer to [8, 9] for the definition of G -stability for multi-step, time-stepping methods.)

Lemma 2 *Let $u(\cdot, t)$ be the mapping from $[0, T]$ to $L^2(\Omega)$, and u_n be the function $u(\cdot, t_n)$ in $L^2(\Omega)$. Assuming the mapping $u(\cdot, t)$ is second-order differentiable in time, then for any $\theta \in [0, 1)$, we have*

$$\|(u_{n+1,\theta} - u_{n,\theta})^2\|^2 \leq C(\theta)(k_n + k_{n-1})^3 \int_{t_{n-1}}^{t_{n+1}} \|u_t\|_{L^4}^4 dt, \tag{10}$$

$$\left\| \frac{u_{n+1,\theta} + u_{n,\theta}}{2} - u(t_{n,\beta}) \right\|^2 \leq C(\theta)(k_n + k_{n-1}) \int_{t_{n-1}}^{t_{n+1}} \|u_t\|^2 dt. \tag{11}$$

When $\theta = 1$, the DLN method reduces to the midpoint rule, and we have

$$\|(u_{n+1,\theta} - u_{n,\theta})^2\|^2 = \|(u_{n+1} - u_n)^2\|^2 \leq Ck_n^3 \int_{t_n}^{t_{n+1}} \|u_t\|_{L^4}^2 dt, \tag{12}$$

$$\left\| \frac{u_{n+1,\theta} + u_{n,\theta}}{2} - u(t_{n,\beta}) \right\|^2 = \left\| \frac{u_{n+1} + u_n}{2} - u\left(\frac{t_{n+1} + t_n}{2}\right) \right\|^2 \leq Ck_n^3 \int_{t_n}^{t_{n+1}} \|u_t\|^2 dt. \tag{13}$$

Under uniform time grids with constant time step k , (11) becomes

$$\left\| \frac{u_{n+1,\theta} + u_{n,\theta}}{2} - u(t_{n,\beta}) \right\|^2 \leq C(\theta)k^3 \int_{t_{n-1}}^{t_{n+1}} \|u_{tt}\|^2 dt. \tag{14}$$

Lemma 3 *Let $u(\cdot, t)$ be the mapping from $[0, T]$ to $H^r(\Omega)$, and u_n be the function $u(\cdot, t_n)$ in $H^r(\Omega)$. Assuming the mapping $u(\cdot, t)$ is third-order differentiable in time, then for any $\theta \in [0, 1)$, we have*

$$\|u_{n,\beta} - u(t_{n,\beta})\|_r^2 \leq C(\theta)(k_n + k_{n-1})^3 \int_{t_{n-1}}^{t_{n+1}} \|u_{ttt}\|_r^2 dt, \tag{15}$$

$$\left\| \frac{u_{n,\alpha}}{\widehat{k}_n} - u_t(t_{n,\beta}) \right\|_r^2 \leq C(\theta)(k_n + k_{n-1})^3 \int_{t_{n-1}}^{t_{n+1}} \|u_{ttt}\|_r^2 dt. \tag{16}$$

When $\theta = 1$, the DLN method reduces to the midpoint rule, and we have

$$\|u_{n,\beta} - u(t_{n,\beta})\|_r^2 = \left\| \frac{u_{n+1} + u_n}{2} - u\left(\frac{t_{n+1} + t_n}{2}\right) \right\|_r^2 \leq Ck_n^3 \int_{t_n}^{t_{n+1}} \|u_{tt}\|_r^2 dt, \tag{17}$$

$$\left\| \frac{u_{n,\alpha}}{\widehat{k}_n} - u_t(t_{n,\beta}) \right\|_r^2 = \left\| \frac{u_{n+1} - u_n}{k_n} - u_t\left(\frac{t_{n+1} + t_n}{2}\right) \right\|_r^2 \leq Ck_n^3 \int_{t_n}^{t_{n+1}} \|u_{ttt}\|_r^2 dt. \tag{18}$$

The proof of these two Lemmas can be found in Appendix A and B.

3 The Modified DLN Algorithm

Let $u_n^h \in X_s^h$ be the numerical approximation of $u(x, t)$ in (1) at time t_n . The modified DLN finite element algorithm for the Allen-Cahn equation (1) is formulated as the following: given $u_{n-1}^h, u_n^h \in X_s^h$, find $u_{n+1}^h \in X_s^h$ such that

$$\left(\frac{u_{n,\alpha}^h}{k_n}, v^h\right) + \epsilon^2(\nabla u_{n,\beta}^h, \nabla v^h) + (\tilde{f}(u_{n+1,\theta}^h, u_{n,\theta}^h), v^h) = 0, \tag{19}$$

holds for all $v^h \in X_s^h$, where $u_{n,\alpha}^h, u_{n,\beta}^h$ and $u_{n,\theta}^h$ are defined in (5) and

$$\begin{aligned} &\tilde{f}(u_{n+1,\theta}^h, u_{n,\theta}^h) \\ &= \frac{1}{4} \left\{ [(u_{n+1,\theta}^h)^3 + (u_{n+1,\theta}^h)^2 u_{n,\theta}^h + u_{n+1,\theta}^h (u_{n,\theta}^h)^2 + (u_{n,\theta}^h)^3] - 2(u_{n+1,\theta}^h + u_{n,\theta}^h) \right\} \\ &= \begin{cases} \frac{F(u_{n+1,\theta}^h) - F(u_{n,\theta}^h)}{u_{n+1,\theta}^h - u_{n,\theta}^h} & \text{if } u_{n+1,\theta}^h \neq u_{n,\theta}^h, \\ f\left(\frac{u_{n+1,\theta}^h + u_{n,\theta}^h}{2}\right) & \text{if } u_{n+1,\theta}^h = u_{n,\theta}^h. \end{cases} \end{aligned}$$

Remark 1 The function $f(u)$ is approximated by \tilde{f} numerically, which has the following properties.

- $\tilde{f}(u, v)$ is continuous and $\partial_u \tilde{f}(u, v), \partial_v \tilde{f}(u, v)$ exist. Note that the solution $u(x, t)$ of the Allen-Cahn model (1) satisfies the maximum principle: if the initial value and boundary conditions are bounded by some constant Γ , then the solution at a later time is also bounded by Γ , i.e.,

$$\|u(\cdot, t)\|_\infty < \Gamma, \quad \forall t > 0.$$

Following the maximum principle, there exists $L > 0$ such that

$$\|f'(u)\|_\infty \leq L,$$

therefore, $\tilde{f}(u, v)$ is Lipschitz-continuous for both components.

- For $\theta \in [0, 1)$, $\tilde{f}(u_{n+1,\theta}, u_{n,\theta})$ is a first order approximation to $f(u(t_n, \beta))$ in time under variable time steps and a second order approximation in time under constant time steps. This can be observed from (11), (14) and

$$\begin{aligned} &\tilde{f}(u_{n+1,\theta}, u_{n,\theta}) - f(u(t_n, \beta)) \\ &= f'(\xi_n) \left(\frac{u_{n+1,\theta} + u_{n,\theta}}{2} - u(t_n, \beta)\right) + \frac{1}{24} f''\left(\frac{u_{n+1,\theta} + u_{n,\theta}}{2}\right) (u_{n+1,\theta} - u_{n,\theta})^2, \end{aligned} \tag{20}$$

which follows from Taylor’s expansion, where ξ_n is between u_n and $u_{n,\beta}$.

For $\theta = 1$, $\tilde{f}(u_{n+1,\theta}, u_{n,\theta})$ is always a second order approximation to $f(u(t_n, \beta))$ in time, which is implied by (13) and (20).

Remark 2 The modified DLN algorithm (19) with $\theta = 1$ reduces to the modified Crank-Nicolson algorithm for the Allen-Cahn equation studied in [48].

Remark 3 Based on the modified DLN method, we can formulate the DLN Convex Splitting scheme (DLN-CSS). As introduced in [48], we split the potential function F into the difference between two convex functions: the implicit part $F_1(u) = \frac{u^4+1}{4}$ and the explicit part

$F_2(u) = \frac{u^2}{2}$. Then we set

$$\widehat{f}(u_{n+1,\theta}^h, u_{n,\theta}^h) = \frac{F_1(u_{n+1,\theta}^{h,IM}) - F_1(u_{n,\theta}^h)}{u_{n+1,\theta}^{h,IM} - u_{n,\theta}^h} - \frac{F_2(u_{n+1,\theta}^{h,EX}) - F_2(u_{n,\theta}^h)}{u_{n+1,\theta}^{h,EX} - u_{n,\theta}^h}, \tag{21}$$

where $u_{n+1,\theta}^{h,IM} = u_{n+1,\theta}^h$ and $u_{n+1,\theta}^{h,EX} = \frac{1+\theta}{2} \left[\left(1 + \frac{k_n}{k_{n-1}}\right) u_n^h - \frac{k_n}{k_{n-1}} u_{n-1}^h \right] + \frac{1-\theta}{2} u_n^h$. The DLN-CSS scheme is obtained by replacing $\widetilde{f}(u_{n+1,\theta}^h, u_{n,\theta}^h)$ in (19) with \widehat{f} in (21).

We test the DLN-CSS scheme on the 1D traveling wave example in Section 6.1. The numerical results are similar to those of the modified DLN scheme, and are omitted to save space.

3.1 Unconditional Stability in Model Energy

We define the corresponding discrete model energy for the modified DLN algorithm (19) at time t_n as

$$\mathcal{E}_n^{\text{MOD}} := \epsilon^2 \left\| \frac{\nabla u_n^h}{\nabla u_{n-1}^h} \right\|_{G(\theta)}^2 + \int_{\Omega} F(u_{n,\theta}^h) dx. \tag{22}$$

The following theorem presents the discrete energy dissipation law satisfied by the numerical solution.

Theorem 1 *The model energy of the variable time-stepping modified DLN algorithm (19) satisfies the discrete energy dissipation law:*

$$\mathcal{E}_{n+1}^{\text{MOD}} \leq \mathcal{E}_n^{\text{MOD}}, \quad n = 1, 2, \dots, N - 1, \tag{23}$$

thus the modified DLN algorithm (19) is unconditionally stable in model energy.

Proof Setting $v^h = u_{n,\alpha}^h (= u_{n+1,\theta}^h - u_{n,\theta}^h)$ in (19) leads to

$$\begin{aligned} & \frac{1}{k_n} \|u_{n,\alpha}^h\|^2 + \epsilon^2 \left\| \frac{\nabla u_{n+1}^h}{\nabla u_n^h} \right\|_{G(\theta)}^2 - \epsilon^2 \left\| \frac{\nabla u_n^h}{\nabla u_{n-1}^h} \right\|_{G(\theta)}^2 + \epsilon^2 \left\| \nabla \left(\sum_{\ell=0}^2 \gamma_\ell^{(n)} u_{n-1+\ell}^h \right) \right\|^2 \\ & + (\widetilde{f}(u_{n+1,\theta}^h, u_{n,\theta}^h), u_{n+1,\theta}^h - u_{n,\theta}^h) = 0, \end{aligned} \tag{24}$$

following the G -stability identity (7). Then we use the fact

$$\widetilde{f}(u_{n+1,\theta}^h, u_{n,\theta}^h)(u_{n+1,\theta}^h - u_{n,\theta}^h) = F(u_{n+1,\theta}^h) - F(u_{n,\theta}^h),$$

to obtain

$$\mathcal{E}_{n+1}^{\text{MOD}} - \mathcal{E}_n^{\text{MOD}} + \frac{1}{k_n} \|u_{n,\alpha}^h\|^2 + \epsilon^2 \left\| \nabla \left(\sum_{\ell=0}^2 \gamma_\ell^{(n)} u_{n-1+\ell}^h \right) \right\|^2 = 0,$$

which implies (23). □

3.2 Error Analysis

This subsection is devoted to the error estimate of the fully discrete modified DLN algorithm (19).

We remind that $\{\beta_\ell^{(n)}\}_{\ell=0}^2$ are uniformly bounded for any fixed $\theta \in [0, 1]$, i.e. $|\beta_\ell^{(n)}| < C_\beta(\theta)$ for all ℓ, n , and define the following discrete Bochner function space for error analysis

$$\ell_\theta^2(0, N; H^r(\Omega)) := \left\{ u(\cdot, t) \in H^r(\Omega) : \|u\|_{\ell_\theta^2(0, N, H^r(\Omega))} = \left(\sum_{n=0}^{N-1} k_n \|u(t_n, \theta)\|_r^2 \right)^{\frac{1}{2}} < \infty \right\}. \tag{25}$$

Theorem 2 Let $u_n^h \in X_s^h$ denote numerical solutions of the modified DLN algorithm in (19) and u_n denote exact solutions of the Allen-Cahn equation in (1) at time t_n . We assume

$$\begin{aligned} u(\cdot, t) &\in H^{s+1}(\Omega), \quad \forall t \in [0, T], \\ u &\in \ell_\theta^2(0, N; H^{s+1}(\Omega)), \quad u_t \in L^2(0, T; H^{s+1}(\Omega)) \cap L^4(0, T; L^4(\Omega)), \\ u_{tt} &\in L^2(0, T; H^1(\Omega)), \quad u_{ttt} \in L^2(0, T; L^2(\Omega)), \end{aligned}$$

there exists $L > 0$ such that $\|f'(u)\|_\infty < L$ for all $t \in [0, T]$, and time step sizes and time step ratios satisfy

$$k_{\max} = \max_{0 \leq n \leq N-1} \{k_n\} < \frac{1}{12\sqrt{3}C_\beta(\theta)L}, \tag{26}$$

$$C_\ell < \frac{k_n}{k_{n-1}} < C_u, \quad n = 1, 2, \dots, N-1, \tag{27}$$

for some $C_\ell, C_u > 0$. Moreover we assume that the initial two solutions u_0^h and u_1^h satisfy

$$\|u_n^h - u_n\| \leq \mathcal{O}(h^{s+1}), \quad n = 0, 1.$$

Then we have: for $\theta \in [0, 1)$

$$\begin{aligned} \max_{0 \leq n \leq N} \{\|u_n^h - u_n\|\} &\leq \mathcal{O}(k_{\max}, h^{s+1}), \\ \left(\frac{\epsilon^2}{2} \sum_{n=1}^{N-1} \widehat{k}_n \|\nabla(u_{n,\beta}^h - u_{n,\beta})\|^2 \right)^{1/2} &\leq \mathcal{O}(k_{\max}, h^s), \end{aligned} \tag{28}$$

and for $\theta = 1$

$$\begin{aligned} \max_{0 \leq n \leq N} \{\|u_n^h - u_n\|\} &\leq \mathcal{O}(k_{\max}^2, h^{s+1}), \\ \left(\frac{\epsilon^2}{2} \sum_{n=1}^{N-1} \widehat{k}_n \|\nabla(u_{n,\beta} - u_{n,\beta}^h)\|^2 \right)^{1/2} &\leq \mathcal{O}(k_{\max}^2, h^s). \end{aligned} \tag{29}$$

Under uniform time grids with constant time step k , (28) becomes

$$\begin{aligned} \max_{0 \leq n \leq N} \{\|u_n^h - u_n\|\} &\leq \mathcal{O}(k^2, h^{s+1}), \\ \left(\frac{\epsilon^2}{2} \sum_{n=1}^{N-1} k \|\nabla(u_{n,\beta} - u_{n,\beta}^h)\|^2 \right)^{1/2} &\leq \mathcal{O}(k^2, h^s). \end{aligned} \tag{30}$$

Proof We start by defining the following Ritz projection operator Π : given $v \in H^1(\Omega)$, $\Pi(v) \in X_s^h$ satisfies

$$(\nabla \Pi(v), \nabla w^h) = (\nabla v, \nabla w^h), \quad (\Pi(v) - v, 1) = 0, \quad \forall w^h \in X_s^h. \tag{31}$$

The following approximation theorem [6, 46] holds for the Ritz projection: for any $v \in H^r(\Omega)$ and its Ritz projection $\Pi(v) \in X_s^h$, we have

$$\|v - \Pi(v)\| + h\|v - \Pi(v)\|_1 \leq Ch^{\min\{r,s+1\}}\|v\|_{\min\{r,s+1\}}. \tag{32}$$

We define the error of u at time t_n to be

$$e_n := u_n - u_n^h = \eta_n + \phi_n^h, \quad \eta_n := u_n - \Pi(u_n), \quad \phi_n^h := \Pi(u_n) - u_n^h.$$

The exact solution u at $t_{n,\beta}$ satisfies

$$(u_t(t_{n,\beta}), v^h) + \epsilon^2(\nabla u(t_{n,\beta}), \nabla v^h) + (f(u(t_{n,\beta})), v^h) = 0, \quad v^h \in X^h. \tag{33}$$

Subtracting (19) from (33) yields

$$\begin{aligned} & \left(\frac{u_{n,\alpha}^h}{\widehat{k}_n} - u_t(t_{n,\beta}), v^h\right) + \epsilon^2(\nabla(u_{n,\beta}^h - u(t_{n,\beta})), \nabla v^h) \\ & \quad + (\widetilde{f}(u_{n+1,\theta}^h, u_{n,\theta}^h) - f(u(t_{n,\beta})), v^h) \\ & = \left(\frac{u_{n,\alpha} - e_{n,\alpha}}{\widehat{k}_n} - u_t(t_{n,\beta}), v^h\right) + \epsilon^2(\nabla(u_{n,\beta} - e_{n,\beta} - u(t_{n,\beta})), \nabla v^h) \\ & \quad + (\widetilde{f}(u_{n+1,\theta}^h, u_{n,\theta}^h) - f(u(t_{n,\beta})), v^h) = 0. \end{aligned} \tag{34}$$

The definition of Π leads to $(\nabla \eta_n, \nabla v^h) = 0$, and (34) can be rewritten as

$$\begin{aligned} & \left(\frac{\phi_{n,\alpha}^h}{\widehat{k}_n}, v^h\right) + \epsilon^2(\nabla \phi_{n,\beta}^h, \nabla v^h) \\ & = \left(\frac{u_{n,\alpha}}{\widehat{k}_n} - u_t(t_{n,\beta}), v^h\right) - \left(\frac{\eta_{n,\alpha}}{\widehat{k}_n}, v^h\right) + \epsilon^2(\nabla(u_{n,\beta} - u(t_{n,\beta})), \nabla v^h) \\ & \quad + (\widetilde{f}(u_{n+1,\theta}^h, u_{n,\theta}^h) - f(u(t_{n,\beta})), v^h). \end{aligned} \tag{35}$$

We set $v^h = \phi_{n,\beta}^h$ in (35) and use the G -stability identity in (7) to obtain

$$\begin{aligned} & \frac{1}{\widehat{k}_n} \left(\left\| \frac{\phi_{n+1}^h}{\phi_n^h} \right\|_{G(\theta)}^2 - \left\| \frac{\phi_n^h}{\phi_{n-1}^h} \right\|_{G(\theta)}^2 + \left\| \sum_{\ell=0}^2 \gamma_\ell^{(n)} \phi_{n-1+\ell}^h \right\|^2 \right) + \epsilon^2 \|\nabla \phi_{n,\beta}^h\|^2 \\ & = \left(\frac{u_{n,\alpha}}{\widehat{k}_n} - u_t(t_{n,\beta}), \phi_{n,\beta}^h\right) - \left(\frac{\eta_{n,\alpha}}{\widehat{k}_n}, \phi_{n,\beta}^h\right) + \epsilon^2(\nabla(u_{n,\beta} - u(t_{n,\beta})), \nabla \phi_{n,\beta}^h) \\ & \quad + (\widetilde{f}(u_{n+1,\theta}^h, u_{n,\theta}^h) - f(u(t_{n,\beta})), \phi_{n,\beta}^h). \end{aligned} \tag{36}$$

Next, we provide a bound for each term on the right-hand side of (36). Utilizing (16), Young’s inequality and the fact $|\beta_\ell^{(n)}| < C_\beta(\theta)$ ($\ell = 0, 1, 2$) leads to

$$\begin{aligned} & \left(\frac{u_{n,\alpha}}{\widehat{k}_n} - u_t(t_{n,\beta}), \phi_{n,\beta}^h\right) \\ & \leq C(\theta, \delta, L) \left\| \frac{u_{n,\alpha}}{\widehat{k}_n} - u_t(t_{n,\beta}) \right\|^2 + \frac{\delta L^2(1+\theta)}{3} (\|\phi_{n+1}^h\|^2 + \|\phi_n^h\|^2 + \|\phi_{n-1}^h\|^2) \\ & \leq C(\theta, \delta, L) k_{\max}^3 \int_{t_{n-1}}^{t_{n+1}} \|u_{ttt}\|^2 dt + \frac{\delta L^2(1+\theta)}{3} (\|\phi_{n+1}^h\|^2 + \|\phi_n^h\|^2 + \|\phi_{n-1}^h\|^2), \end{aligned} \tag{37}$$

where $\delta > 0$ will be decided later and $C(\theta, \delta, L)$ is a constant only depending on θ, δ, L . By Cauchy-Schwarz inequality, Young’s inequality and the projection error (32)

$$\begin{aligned} \frac{1}{\widehat{k}_n}(\eta_{n,\alpha}, \phi_{n,\beta}^h) &\leq \frac{C(\theta, \delta, L)}{\widehat{k}_n^2} \|\eta_{n,\alpha}\|^2 + \frac{\delta L^2(1+\theta)}{3} (\|\phi_{n+1}^h\|^2 + \|\phi_n^h\|^2 + \|\phi_{n-1}^h\|^2) \\ &\leq \frac{C(\theta, \delta, L)h^{2s+2}}{\widehat{k}_n^2} \|u_{n,\alpha}\|_{s+1}^2 + \frac{\delta L^2(1+\theta)}{3} (\|\phi_{n+1}^h\|^2 + \|\phi_n^h\|^2 + \|\phi_{n-1}^h\|^2) \\ &\leq \frac{C(\theta, \delta, L)h^{2s+2}}{\widehat{k}_n^2} (\|u_{n+1} - u_n\|_{s+1}^2 + \|u_n - u_{n-1}\|_{s+1}^2) \\ &\quad + \frac{\delta L^2(1+\theta)}{3} (\|\phi_{n+1}^h\|^2 + \|\phi_n^h\|^2 + \|\phi_{n-1}^h\|^2). \end{aligned} \tag{38}$$

By Hölder’s inequality, we have

$$\|u_{n+1} - u_n\|_{s+1}^2 \leq \left\| \int_{t_n}^{t_{n+1}} u_t(\cdot, t) dt \right\|_{s+1}^2 \leq k_n \int_{t_n}^{t_{n+1}} \|u_t\|_{s+1}^2 dt, \tag{39}$$

therefore, (38) becomes

$$\begin{aligned} \frac{1}{\widehat{k}_n}(\eta_{n,\alpha}, \phi_{n,\beta}^h) &\leq \frac{C(\delta, \theta, L)h^{2s+2}}{\widehat{k}_n} \int_{t_{n-1}}^{t_{n+1}} \|u_t\|_{s+1}^2 dt \\ &\quad + \frac{\delta L^2(1+\theta)}{3} (\|\phi_{n+1}^h\|^2 + \|\phi_n^h\|^2 + \|\phi_{n-1}^h\|^2). \end{aligned} \tag{40}$$

By Cauchy-Schwarz inequality and (15)

$$\begin{aligned} \epsilon^2 \left(\nabla(u_{n,\beta} - u(t_{n,\beta})), \nabla\phi_{n,\beta}^h \right) &\leq \epsilon^2 \left\| \nabla(u_{n,\beta} - u(t_{n,\beta})) \right\| \left\| \nabla\phi_{n,\beta}^h \right\| \\ &\leq C(\theta)\epsilon^2 k_{\max}^3 \int_{t_{n-1}}^{t_{n+1}} \|\nabla u_{tt}\|^2 dt + \frac{\epsilon^2}{2} \|\nabla\phi_{n,\beta}^h\|^2. \end{aligned} \tag{41}$$

For the non-linear term, utilizing Cauchy Schwarz inequality, triangle inequality and Young’s inequality leads to

$$\begin{aligned} &\left(\widetilde{f}(u_{n+1,\theta}^h, u_{n,\theta}^h) - f(u(t_{n,\beta})), \phi_{n,\beta}^h \right) \\ &\leq C_\beta(\theta) \|\widetilde{f}(u_{n+1,\theta}^h, u_{n,\theta}^h) - f(u(t_{n,\beta}))\| (\|\phi_{n+1}^h\| + \|\phi_n^h\| + \|\phi_{n-1}^h\|) \\ &\leq \frac{9C_\beta^2(\theta)}{4\delta L^2(1+\theta)} \|\widetilde{f}(u_{n+1,\theta}^h, u_{n,\theta}^h) - f(u(t_{n,\beta}))\|^2 \\ &\quad + \frac{\delta L^2(1+\theta)}{9} (\|\phi_{n+1}^h\| + \|\phi_n^h\| + \|\phi_{n-1}^h\|)^2 \\ &\leq \frac{9C_\beta^2(\theta)}{4\delta L^2(1+\theta)} \|\widetilde{f}(u_{n+1,\theta}^h, u_{n,\theta}^h) - f(u(t_{n,\beta}))\|^2 \\ &\quad + \frac{\delta L^2(1+\theta)}{3} (\|\phi_{n+1}^h\|^2 + \|\phi_n^h\|^2 + \|\phi_{n-1}^h\|^2). \end{aligned} \tag{42}$$

Considering the first term on the right-hand side, we have

$$\begin{aligned} \|\widetilde{f}(u_{n+1,\theta}^h, u_{n,\theta}^h) - f(u(t_{n,\beta}))\|^2 &\leq 3\|\widetilde{f}(u_{n+1,\theta}^h, u_{n,\theta}^h) - \widetilde{f}(u_{n+1,\theta}, u_{n,\theta}^h)\|^2 \\ &\quad + 3\|\widetilde{f}(u_{n+1,\theta}, u_{n,\theta}^h) - \widetilde{f}(u_{n+1,\theta}, u_{n,\theta})\|^2 + 3\|\widetilde{f}(u_{n+1,\theta}, u_{n,\theta}) - f(u(t_{n,\beta}))\|^2. \end{aligned} \tag{43}$$

By the assumption $\|f'(u)\|_\infty < L$, $\tilde{f}(\cdot, \cdot)$ are Lipschitz-continuous for both components [42]. Thus

$$\begin{aligned} & \|\tilde{f}(u_{n+1,\theta}^h, u_{n,\theta}^h) - \tilde{f}(u_{n+1,\theta}, u_{n,\theta}^h)\|^2 \leq L^2 \|u_{n+1,\theta}^h - u_{n+1,\theta}\|^2 \\ & \leq L^2 \|\eta_{n+1,\theta} + \phi_{n+1,\theta}^h\|^2 \leq CL^2 h^{2s+2} \|u_{n+1,\theta}\|_{s+1}^2 + 2L^2 \|\phi_{n+1,\theta}^h\|^2 \\ & \leq CL^2 h^{2s+2} (\|u_{n+1,\theta} - u(t_{n+1,\theta})\|_{s+1}^2 + \|u(t_{n+1,\theta})\|_{s+1}^2) + 2L^2 \|\phi_{n+1,\theta}^h\|^2 \\ & \leq C(\theta, L) h^{2s+2} \left(k_n \int_{t_n}^{t_{n+1}} \|u_t\|_{s+1}^2 dt + \|u(t_{n+1,\theta})\|_{s+1}^2 \right) \\ & \quad + (1 + \theta)^2 L^2 (\|\phi_{n+1}^h\|^2 + \|\phi_n^h\|^2), \end{aligned} \tag{44}$$

where the last inequality follows from Hölder’s inequality as in (39). Similarly, we have

$$\begin{aligned} & \|\tilde{f}(u_{n+1,\theta}, u_{n,\theta}^h) - \tilde{f}(u_{n+1,\theta}, u_{n,\theta})\|^2 \\ & \leq C(\theta, L) h^{2s+2} \left(k_{n-1} \int_{t_{n-1}}^{t_n} \|u_t\|_{s+1}^2 dt + \|u(t_{n,\theta})\|_{s+1}^2 \right) + (1 + \theta)^2 L^2 (\|\phi_n^h\|^2 + \|\phi_{n-1}^h\|^2). \end{aligned} \tag{45}$$

We use (10)-(11) in Lemma 2 and (20) to obtain

$$\begin{aligned} & \|\tilde{f}(u_{n+1,\theta}, u_{n,\theta}) - f(u(t_{n,\beta}))\|^2 \\ & \leq C(L) \left\| \frac{u_{n+1,\theta} + u_{n,\theta}}{2} - u(t_{n,\beta}) \right\|^2 + C \|u_{n+1,\theta} - u_{n,\theta}\|^2 \\ & \leq C(\theta, L) (k_n + k_{n-1}) \int_{t_{n-1}}^{t_{n+1}} \|u_t\|^2 dt + C(\theta) (k_n + k_{n-1})^3 \int_{t_{n-1}}^{t_{n+1}} \|u_t\|_{L^4}^4 dt. \end{aligned} \tag{46}$$

Combining (42) - (46), we have

$$\begin{aligned} & \left(\tilde{f}(u_{n+1,\theta}^h, u_{n,\theta}^h) - f(u(t_{n,\beta})) \right), \phi_{n,\beta}^h \Big) \\ & \leq C(\theta, \delta, L) h^{2s+2} \left(k_{\max} \int_{t_{n-1}}^{t_{n+1}} \|u_t\|_{s+1}^2 dt + \|u(t_{n+1,\theta})\|_{s+1}^2 + \|u(t_{n,\theta})\|_{s+1}^2 \right) \\ & \quad + C(\theta, \delta, L) k_{\max} \int_{t_{n-1}}^{t_{n+1}} \|u_t\|^2 dt + C(\theta, \delta, L) k_{\max}^3 \int_{t_{n-1}}^{t_{n+1}} \|u_t\|_{L^4}^4 dt \\ & \quad + \frac{27(1 + \theta)C_\beta^2(\theta)}{4\delta} (\|\phi_{n+1}^h\|^2 + 2\|\phi_n^h\|^2 + \|\phi_{n-1}^h\|^2) \\ & \quad + \frac{\delta L^2(1 + \theta)}{3} (\|\phi_{n+1}^h\|^2 + \|\phi_n^h\|^2 + \|\phi_{n-1}^h\|^2). \end{aligned} \tag{47}$$

Now, we are ready to derive the error estimate. We combine (36), (37), (40), (41) and (47), multiply both sides by \widehat{k}_n and use the time ratio condition in (27) to obtain

$$\begin{aligned} & \left\| \phi_{n+1}^h \right\|_{G(\theta)}^2 - \left\| \phi_n^h \right\|_{G(\theta)}^2 + \left\| \sum_{\ell=0}^2 \gamma_\ell^{(n)} \phi_{n-1+\ell}^h \right\|^2 + \frac{\epsilon^2}{2} \widehat{k}_n \|\nabla \phi_{n,\beta}^h\|^2 \\ & \leq (1 + \theta) \left(\frac{27C_\beta^2(\theta)}{4\delta} + \delta L^2 \right) \widehat{k}_n (\|\phi_{n+1}^h\|^2 + 2\|\phi_n^h\|^2 + \|\phi_{n-1}^h\|^2) \\ & \quad + C(\theta, \delta, L) k_{\max}^4 \int_{t_{n-1}}^{t_{n+1}} \|u_{ttt}\|^2 dt + C(\delta, \theta, L) h^{2s+2} \int_{t_{n-1}}^{t_{n+1}} \|u_t\|_{s+1}^2 dt \end{aligned}$$

$$\begin{aligned}
 &+ C(\theta)\epsilon^2 k_{\max}^4 \int_{t_{n-1}}^{t_{n+1}} \|\nabla u_{tt}\|^2 dt + C(\theta, \delta, L)h^{2s+2}k_{\max}^2 \int_{t_{n-1}}^{t_{n+1}} \|u_t\|_{s+1}^2 dt \\
 &+ C(\theta, \delta, L)h^{2s+2}(\widehat{k}_n \|u(t_{n+1}, \theta)\|_{s+1}^2 + \widehat{k}_n \|u(t_n, \theta)\|_{s+1}^2) \\
 &+ C(\theta, \delta, L)k_{\max}^2 \int_{t_{n-1}}^{t_{n+1}} \|u_t\|^2 dt + C(\theta, \delta, L)k_{\max}^4 \int_{t_{n-1}}^{t_{n+1}} \|u_t\|_{L^4}^4 dt, \tag{48}
 \end{aligned}$$

We sum (48) over n from 1 to $N - 1$, use the definition of $G(\theta)$ -norm in (8), drop the non-negative term $\|\phi_{N-1}^h\|^2$, $\|\sum_{\ell=0}^2 \gamma_\ell^{(n)} \phi_{n-1+\ell}^h\|^2$ and use the time ratio condition in (27) to obtain

$$\begin{aligned}
 &\left[\frac{1+\theta}{4} - (1+\theta)\left(\frac{27C_\beta^2(\theta)}{4\delta} + \delta L^2\right)k_{\max} \right] \|\phi_N^h\|^2 + \frac{\epsilon^2}{2} \sum_{n=1}^{N-1} \widehat{k}_n \|\nabla \phi_{n,\beta}^h\|^2 \\
 &\leq C(\theta, \delta, L, C_\ell, C_u) \sum_{n=0}^{N-1} k_n \|\phi_n^h\|^2 + C(\theta, \delta, L)k_{\max}^4 \|u_{ttt}\|_{L^2(0,T;L^2)}^2 \\
 &\quad + C(\delta, \theta, L)h^{2s+2}(1+k_{\max}^2) \|u_t\|_{L^2(0,T;H^{s+1})}^2 + C(\theta)\epsilon^2 k_{\max}^4 \|\nabla u_{tt}\|_{L^2(0,T;L^2)}^2 \\
 &\quad + C(\theta, \delta, L, C_\ell, C_u)h^{2s+2} \|u\|_{\ell_0^2(0,N;H^{s+1})}^2 + C(\theta, \delta, L)k_{\max}^2 \|u_t\|_{L^2(0,T;L^2)}^2 \\
 &\quad + C(\theta, \delta, L)k_{\max}^4 \|u_t\|_{L^4(0,T;L^4)}^4 + \frac{1+\theta}{4} \|\phi_1^h\|^2 + \frac{1-\theta}{4} \|\phi_0^h\|^2. \tag{49}
 \end{aligned}$$

To estimate $\|\phi_N^h\|^2$, we need

$$\frac{1+\theta}{4} - (1+\theta)\left(\frac{27C_\beta^2(\theta)}{4\delta} + \delta L^2\right)k_{\max} > 0.$$

We set $\delta = \frac{3\sqrt{3}C_\beta(\theta)}{2L}$ to relax the upper bound for k_{\max} and obtain the time step restriction in (26). By the discrete Gronwall inequality [23] and the fact that the maximum time step $k_{\max} < 1$, we have

$$\begin{aligned}
 &\|\phi_N^h\|^2 + \frac{\epsilon^2 C(\theta, L)}{2} \sum_{n=1}^{N-1} \widehat{k}_n \|\nabla \phi_{n,\beta}^h\|^2 \\
 &\leq \exp\left(C(\theta, L, C_\ell, C_u)T\right) \left\{ C(\theta, L)k_{\max}^4 \|u_{ttt}\|_{L^2(0,T;L^2)}^2 + C(\theta, L)h^{2s+2} \|u_t\|_{L^2(0,T;H^{s+1})}^2 \right. \\
 &\quad + C(\theta)\epsilon^2 k_{\max}^4 \|\nabla u_{tt}\|_{L^2(0,T;L^2)}^2 + C(\theta, L)k_{\max}^2 \|u_t\|_{L^2(0,T;L^2)}^2 \\
 &\quad + C(\theta, L, C_\ell, C_u)h^{2s+2} \|u\|_{\ell_0^2(0,N;H^{s+1})}^2 + C(\theta, L)k_{\max}^4 \|u_t\|_{L^4(0,T;L^4)}^4 \\
 &\quad \left. + C(\theta)(\|\phi_1^h\|^2 + \|\phi_0^h\|^2) \right\}, \tag{50}
 \end{aligned}$$

which leads to

$$\begin{aligned}
 &\|\phi_N^h\| + \left(\frac{\epsilon^2}{2} \sum_{n=1}^{N-1} \widehat{k}_n \|\nabla \phi_{n,\beta}^h\|^2\right)^{1/2} \\
 &\leq C(\theta, L, T, C_\ell, C_u) \left\{ k_{\max}^2 \|u_{ttt}\|_{L^2(0,T;L^2)} + h^{s+1} \|u_t\|_{L^2(0,T;H^{s+1})} + \epsilon k_{\max}^2 \|\nabla u_{tt}\|_{L^2(0,T;L^2)} \right. \\
 &\quad + k_{\max} \|u_t\|_{L^2(0,T;L^2)} + h^{s+1} \|u\|_{\ell_0^2(0,N;H^{s+1})} + k_{\max}^2 \|u_t\|_{L^4(0,T;L^4)} \\
 &\quad \left. + \|\phi_1^h\| + \|\phi_0^h\| \right\}. \tag{51}
 \end{aligned}$$

By (51), triangle inequality and (32), we have (28).

Lastly, we comment on the case of uniform time grids with constant time step k . Under such case, utilizing (10) and (14) in Lemma 2, Eq. (46) becomes

$$\begin{aligned} & \|\tilde{f}(u_{n+1,\theta}, u_{n,\theta}) - f(u(t_n,\beta))\|^2 \\ & \leq C(L) \left\| \frac{u_{n+1,\theta} + u_{n,\theta}}{2} - u(t_n,\beta) \right\|^2 + C \|u_{n+1,\theta} - u_{n,\theta}\|^2 \\ & \leq C(\theta, L)k^3 \int_{t_{n-1}}^{t_{n+1}} \|u_{tt}\|^2 dt + C(\theta)k^3 \int_{t_{n-1}}^{t_{n+1}} \|u_t\|_{L^4}^4 dt. \end{aligned}$$

Following similar arguments, we have (30). □

Remark 4 We have proven that the modified DLN algorithm is first-order accurate in time under arbitrary time step sequences. However, all numerical tests in Section 6 demonstrate that numerical solutions on both uniform and non-uniform time grids converge at second-order in time.

4 The DLN-SAV algorithm

In this section, we consider the energy-stable SAV approach, and present the DLN-SAV algorithm. For the Allen-Cahn model (1), we introduce the scalar auxiliary variable of the form

$$r(t) = \sqrt{E(u(x, t)) + C_0},$$

with

$$E(u(x, t)) = \int_{\Omega} \left(F(u(x, t)) - \frac{\lambda}{2} u^2(x, t) \right) dx,$$

where $\lambda > 0$ is a small positive number and $C_0 > 0$ is picked to ensure $r(t) > C_r > 0$ for some constant C_r . Then the Allen-Cahn model in (1) can be equivalently written as

$$\begin{cases} u_t - \epsilon^2 \Delta u + \lambda u + \frac{r}{\sqrt{E(u) + C_0}} g(u) = 0, & x \in \Omega, 0 < t \leq T, \\ r_t = \frac{1}{2\sqrt{E(u) + C_0}} \int_{\Omega} g(u) u_t dx, & 0 < t \leq T. \end{cases} \tag{52}$$

where $g(u) = f(u) - \lambda u$.

4.1 The algorithm

Let u_n^h, r_n^h be fully-discrete numerical solutions of $u(x, t_n), r(t_n)$ respectively. The fully-discrete weak formulation for the DLN-SAV algorithm with the finite element spatial discretization is: given $u_{n-1}^h, u_n^h \in X_s^h$ and r_{n-1}^h, r_n^h , we find $u_{n+1}^h \in X_s^h$ and r_{n+1}^h such that for all $v^h \in X_s^h$

$$\begin{cases} \left(\frac{u_{n,\alpha}^h}{\widehat{k}_n}, v^h \right) + \epsilon^2 (\nabla u_{n,\beta}^h, \nabla v^h) + \lambda (u_{n,\beta}^h, v^h) + \frac{r_{n,\beta}^h}{\sqrt{E(u_{n,*}^h) + C_0}} (g(u_{n,*}^h), v^h) = 0, \\ \frac{r_{n,\alpha}^h}{\widehat{k}_n} = \frac{1}{2\sqrt{E(u_{n,*}^h) + C_0}} \left(g(u_{n,*}^h), \frac{u_{n,\alpha}^h}{\widehat{k}_n} \right), \end{cases} \tag{53}$$

where $u_{n,*}^h$ defined in (6) is the explicit second-order approximation to $u(t_n, \beta)$ in time.

The variable time-stepping DLN scheme can be simplified by the refactorization process: adding a few lines of codes to the *backward Euler (BE) scheme* to obtain the DLN solutions (see [28] for details). The DLN-SAV algorithm can be equivalently rewritten as the following process:

Step 1. Pre-process

$$k_n^{\text{BE}} = b^{(n)} \widehat{k}_n, \quad u_n^{h,\text{old}} = a_1^{(n)} u_n^h + a_0^{(n)} u_{n-1}^h \in X_s^h, \quad r_n^{h,\text{old}} = a_1^{(n)} r_n^h + a_0^{(n)} r_{n-1}^h,$$

where the coefficients for the pre-process are

$$a_1^{(n)} = \beta_1^{(n)} - \alpha_1 \beta_2^{(n)} / \alpha_2, \quad a_0^{(n)} = \beta_0^{(n)} - \alpha_0 \beta_2^{(n)} / \alpha_2, \quad b^{(n)} = \beta_2^{(n)} / \alpha_2.$$

Step 2. BE solver to solve $u_{n+1}^{h,\text{temp}} \in X_s^h$ and $r_{n+1}^{h,\text{temp}}$ such that for all $v^h \in X_s^h$

$$\begin{cases} \left(\frac{u_{n+1}^{h,\text{temp}} - u_n^{h,\text{old}}}{k_n^{\text{BE}}}, v^h \right) + \epsilon^2 (\nabla u_{n+1}^{h,\text{temp}}, \nabla v^h) + \lambda (u_{n+1}^{h,\text{temp}}, v^h) \\ \quad + \frac{r_{n+1}^{h,\text{temp}}}{\sqrt{E(u_{n,*}^h) + C_0}} (g(u_{n,*}^h), v^h) = 0, \\ \frac{r_{n+1}^{h,\text{temp}} - r_n^{h,\text{old}}}{k_n^{\text{BE}}} = \frac{1}{2\sqrt{E(u_{n,*}^h) + C_0}} \left(g(u_{n,*}^h), \frac{u_{n+1}^{h,\text{temp}} - u_n^{h,\text{old}}}{k_n^{\text{BE}}} \right). \end{cases} \tag{54}$$

Step 3. Post-process

$$u_{n+1}^h = c_2^{(n)} u_{n+1}^{h,\text{temp}} + c_1^{(n)} u_n^h + c_0^{(n)} u_{n-1}^h, \quad r_{n+1}^h = c_2^{(n)} r_{n+1}^{h,\text{temp}} + c_1^{(n)} r_n^h + c_0^{(n)} r_{n-1}^h,$$

where the coefficients for the post-process are

$$c_2^{(n)} = 1/\beta_2^{(n)}, \quad c_1^{(n)} = -\beta_1^{(n)}/\beta_2^{(n)}, \quad c_0^{(n)} = -\beta_0^{(n)}/\beta_2^{(n)}.$$

In practice, the scalar auxiliary variable r need not be refactorized in Step 3, since its effect on accuracy can be negligible [53]. The above refactorization process can be applied to the modified DLN algorithm in (19) as well. However, the refactorization process of the modified DLN algorithm does not simplify the implementation much since the partially implicit, non-linear term needs to be refactorized as well, and was omitted in Section 3.

Lemma 4 *The DLN-SAV algorithm in (53) admits a unique solution.*

Proof Since the DLN-SAV algorithm in (53) is equivalent to the above refactorization process, it suffices to show that the BE solver in (54) has a unique solution. We denote

$$\varphi_n^h = \frac{g(u_{n,*}^h)}{\sqrt{E(u_{n,*}^h) + C_0}},$$

and eliminate $r_{n+1}^{h,\text{temp}}$ in (54) to obtain

$$\begin{aligned} & (u_{n+1}^{h,\text{temp}}, v^h) + \epsilon^2 k_n^{\text{BE}} (\nabla u_{n+1}^{h,\text{temp}}, \nabla v^h) + \lambda k_n^{\text{BE}} (u_{n+1}^{h,\text{temp}}, v^h) \\ & \quad + \frac{1}{2} k_n^{\text{BE}} (u_{n+1}^{h,\text{temp}}, \varphi_n^h) (\varphi_n^h, v^h) = (u_n^h, v^h), \\ & w_n^h = u_n^{h,\text{old}} + \frac{1}{2} k_n^{\text{BE}} (u_n^{h,\text{old}}, \varphi_n^h) \varphi_n^h - k_n^{\text{BE}} r_n^{h,\text{old}} \varphi_n^h. \end{aligned} \tag{55}$$

Let $\{\psi_\ell\}_{\ell=1}^{N_d}$ be the basis for X_s^h . We have $u_{n+1}^{h, \text{temp}} = \sum_{\ell=1}^{N_d} U_\ell^{(n+1)} \psi_\ell$ for some coordinates $\{U_\ell^{(n+1)}\}_{\ell=1}^{N_d}$. We define the matrices $M, K \in \mathbb{R}^{N_d \times N_d}$ as

$$M = [M_{ij}]_{N_d \times N_d} = [(\psi_j, \psi_i)]_{N_d \times N_d}, \quad K = [K_{ij}]_{N_d \times N_d} = [(\nabla \psi_j, \nabla \psi_i)]_{N_d \times N_d},$$

and vectors $B^{(n)}, U^{(n+1)}, W^{(n)} \in \mathbb{R}^{N_d \times 1}$ as

$$B^{(n)} = [B_i^{(n)}]_{N_d \times 1} = [(\varphi_n^h, \psi_i)]_{N_d \times 1}, \quad U^{(n+1)} = [U_i^{(n+1)}]_{N_d \times 1},$$

$$W^{(n)} = [W_i^{(n)}]_{N_d \times 1} = [(w_n^h, \psi_i)]_{N_d \times 1}.$$

Then the algebraic structure for (55) is

$$[(1 + \lambda k_n^{\text{BE}})M + \epsilon^2 k_n^{\text{BE}} K + \frac{1}{2} k_n^{\text{BE}} B^{(n)} (B^{(n)})^T] U^{(n+1)} = W^{(n)}. \tag{56}$$

Since the mass matrix $M > 0$, the stiffness matrix $K \geq 0$ and $B^{(n)} (B^{(n)})^T \geq 0$, the linear system in (56) has a unique solution. In addition, $r_{n+1}^{h, \text{temp}}$ is uniquely obtained from the second equation of (54). \square

4.2 Numerical implementation

The left matrix in (56) is far away from a sparse matrix. To efficiently implement the DLN-SAV scheme, we solve (55) in the following simpler way. We denote $A = I - \epsilon^2 k_n^{\text{BE}} \Delta > 0$ and apply integration by parts to (55) to rewrite it as

$$(Au_{n+1}^{h, \text{temp}}, v^h) + \frac{k_n^{\text{BE}}}{2} (u_{n+1}^{h, \text{temp}}, \varphi_n^h) (\varphi_n^h, v^h) = (w_n^h, v^h), \quad \forall v^h \in X_s^h. \tag{57}$$

To solve $u_{n+1}^{h, \text{temp}}$ in (57) efficiently, we first solve for $(u_{n+1}^{h, \text{temp}}, \varphi_n^h)$. Given any function $G \in (H^{-1}(\Omega))^d$, we define $A^{-1}G \in X_s^h$ to be the unique finite element solution to the following second-order system

$$\begin{cases} u - \epsilon^2 k_n^{\text{BE}} \Delta u = G, & x \in \Omega, \\ \frac{\partial u}{\partial n} = 0, & \text{on } \partial\Omega. \end{cases}$$

Thus $A^{-1}G \in X_s^h$ satisfies the following weak form

$$\begin{cases} (A(A^{-1}G), v^h) = (G, v^h), \\ (\frac{\partial}{\partial n} (A^{-1}G), v^h)_{\partial\Omega} = 0, \end{cases} \quad \forall v^h \in X_s^h. \tag{58}$$

We use the definition (58) and integration by parts to obtain

$$(Au_{n+1}^{h, \text{temp}}, A^{-1}\varphi_n^h) = (u_{n+1}^{h, \text{temp}}, A(A^{-1}\varphi_n^h)) = (u_{n+1}^{h, \text{temp}}, \varphi_n^h),$$

$$(w_n^h, A^{-1}\varphi_n^h) = (A(A^{-1}w_n^h), A^{-1}\varphi_n^h) = (A^{-1}w_n^h, A(A^{-1}\varphi_n^h)) = (A^{-1}w_n^h, \varphi_n^h) \tag{59}$$

We use (59) and set $v^h = A^{-1}\varphi_n^h$ in (57) to solve

$$(u_{n+1}^{h, \text{temp}}, \varphi_n^h) = \frac{(A^{-1}w_n^h, \varphi_n^h)}{1 + \frac{k_n^{\text{BE}}}{2} (A^{-1}\varphi_n^h, \varphi_n^h)}. \tag{60}$$

To obtain $u_{n+1}^{h, \text{temp}}$ from (57), it suffices to solve

$$Au_{n+1}^{h, \text{temp}} + \frac{k_n^{\text{BE}}}{2}(u_{n+1}^{h, \text{temp}}, \varphi_n^h)\varphi_n^h = w_n^h,$$

or equivalently,

$$u_{n+1}^{h, \text{temp}} = -\frac{k_n^{\text{BE}}}{2}(u_{n+1}^{h, \text{temp}}, \varphi_n^h)A^{-1}\varphi_n^h + A^{-1}w_n^h. \tag{61}$$

We summarize the simplified implementation in the following steps.

(i) Solving for $A^{-1}\varphi_n^h \in X_s^h$ via

$$(A^{-1}\varphi_n^h, v^h) + \epsilon^2 k_n^{\text{BE}}(\nabla(A^{-1}\varphi_n^h), \nabla v^h) = (\varphi_n^h, v^h), \quad \forall v^h \in X_s^h. \tag{62}$$

(ii) Solving for $A^{-1}w_n^h \in X_s^h$ via

$$(A^{-1}w_n^h, v^h) + \epsilon^2 k_n^{\text{BE}}(\nabla(A^{-1}w_n^h), \nabla v^h) = (w_n^h, v^h), \quad \forall v^h \in X_s^h. \tag{63}$$

(iii) Computing $(u_{n+1}^{h, \text{temp}}, \varphi_n^h)$ by (60).

(iv) Computing $u_{n+1}^{h, \text{temp}}$ from (61) and $r_{n+1}^{h, \text{temp}}$ from the second equation of (54).

Remark 5 It is straightforward to verify that the solution pair $(u_{n+1}^{h, \text{temp}}, r_{n+1}^{h, \text{temp}})$ obtained by the above process is the unique solution to the algorithm in (54), and the details are omitted here.

Remark 6 Solving two second-order equations in (62) and (63) is much more efficient than solving (56) directly since the left matrix of the two linear systems in (62) and (63) becomes a sparse matrix $M + \epsilon^2 k_n^{\text{BE}} K$.

4.3 Unconditional Stability in Model Energy

We define the discrete model energy for the DLN-SAV algorithm (53) at time t_n as

$$\mathcal{E}_n^{\text{SAV}} = \epsilon^2 \left\| \frac{\nabla u_n^h}{\nabla u_{n-1}^h} \right\|_{G(\theta)}^2 + \lambda \left\| \frac{u_n^h}{u_{n-1}^h} \right\|_{G(\theta)}^2 + \frac{1+\theta}{2}(r_n^h)^2 + \frac{1-\theta}{2}(r_{n-1}^h)^2, \tag{64}$$

and have the following theorem on its unconditional stability with respect to $\mathcal{E}_n^{\text{SAV}}$.

Theorem 3 *The model energy of the variable time-stepping DLN-SAV algorithm (53) satisfies:*

$$\mathcal{E}_{n+1}^{\text{SAV}} \leq \mathcal{E}_n^{\text{SAV}}, \quad n = 1, 2, \dots, N-1, \tag{65}$$

thus the DLN-SAV algorithm is unconditionally stable with respect to this model energy.

Proof We set $v^h = u_{n,\alpha}^h$ in the first equation of the DLN-SAV algorithm (53)

$$\frac{\|u_{n,\alpha}^h\|^2}{\widehat{k}_n} + \epsilon^2(\nabla u_{n,\beta}^h, \nabla u_{n,\alpha}^h) + \lambda(u_{n,\beta}^h, u_{n,\alpha}^h) + \frac{r_{n,\beta}^h}{\sqrt{E(u_{n,*}^h) + C_0}}(g(u_{n,*}^h), u_{n,\alpha}^h) = 0. \tag{66}$$

We multiply the second equation of the DLN-SAV algorithm (53) by $\widehat{2k}_n r_{n,\beta}$ and obtain

$$2r_{n,\alpha}^h r_{n,\beta}^h = \frac{r_{n,\beta}^h}{\sqrt{E(u_{n,*}^h) + C_0}}(g(u_{n,*}^h), u_{n,\alpha}^h). \tag{67}$$

We combine (66) and (67) and use the G -stability identity (7) to obtain

$$\frac{1}{k_n} \|u_{n,\alpha}^h\|^2 + \mathcal{E}_{n+1}^{\text{SAV}} - \mathcal{E}_n^{\text{SAV}} + \epsilon^2 \left\| \nabla \left(\sum_{\ell=0}^2 \gamma_\ell^{(n)} u_{n-1+\ell}^h \right) \right\|^2 + \lambda \left\| \sum_{\ell=0}^2 \gamma_\ell^{(n)} u_{n-1+\ell}^h \right\|^2 + 2 \left(\sum_{\ell=0}^2 \gamma_\ell^{(n)} r_{n-1+\ell}^h \right)^2 = 0, \tag{68}$$

which results in the unconditional stability property (65). □

Remark 7 The inequality in (65) is the discrete version of the energy dissipation law (2) and the discrete energy $\mathcal{E}_n^{\text{SAV}}$ in (64) is an approximation of the model energy \mathcal{E} .

4.4 Error Analysis

In this subsection, we investigate the error estimate of the fully discrete DLN-SAV algorithm (53). Let u_n, r_n be exact solutions $u(x, t), r(t)$ evaluated at t_n respectively. The errors of numerical solutions of the DLN-SAV algorithm in (53) at time t_n are denoted as

$$e_n^u = u_n - u_n^h, \quad e_n^r = r_n - r_n^h.$$

Introduce the following discrete Bochner function space for error analysis

$$\begin{aligned} & \ell_\beta^2(0, N; H^{s+1}(\Omega)) \\ & := \left\{ u(\cdot, t) \in L^2(\Omega) : \|u\|_{\ell_\beta^2(0, N; H^{s+1}(\Omega))} = \left(\sum_{n=1}^{N-1} (k_n + k_{n-1}) \|u(t_{n,\beta})\|_{s+1}^2 \right)^{\frac{1}{2}} < \infty \right\}. \end{aligned} \tag{69}$$

Since $t_{n,\beta}$ is a point between t_{n-1} and t_{n+1} , the above discrete norm can be understood as the Riemann sum of $\sqrt{2} \|u\|_{L^2(0, T; L^2(\Omega))}$.

To carry out the error analysis, one key idea is to use the mathematical induction to prove the following statement

$$\|e_M^u\| \leq Ch, \tag{70}$$

for any M between 0 and N , under certain time step assumptions. To start, we assume that (70) holds for $n = 0, 1, \dots, M - 1$. Since the exact solution u satisfies the maximum principle and is bounded, it can be derived that $\{\|u_n^h\|_\infty\}_{n=0}^{M-1}$ uniformly bounded following the triangle inequality. Next, we use the Ritz projection operator to decompose the error e_n^u as

$$e_n^u = (u_n - \Pi(u_n)) + (\Pi(u_n) - u_n^h) = \eta_n + \phi_n^h.$$

Applying inverse inequality, triangle inequality and approximation theorem in (32) leads to

$$\|\phi_n^h\|_\infty \leq Ch^{-1/2} \|\phi_n^h\| \leq Ch^{-1/2} (\|e_n^u\| + \|\eta_n\|) \leq Ch^{1/2}.$$

Thus for $n = 0, 1, \dots, M - 1$, $\|e_n^u\|_\infty \leq Ch^{1/2}$ and $\sqrt{E(u_{n,*}^h) + C_0} > C_r/2$ if exact solutions satisfy $\sqrt{E(u_{n,*}) + C_0} > C_r$ and the diameter h is small enough.

Then we combine all these facts to achieve

$$\|e_M^u\| + \|\nabla e_M^u\| \leq \mathcal{O}(k_{\max}^2, h^s), \tag{71}$$

which will be summarized in Theorem 4 below. Therefore, we can verify (70) for $n = M$ under the time step restriction $k_{\max} \leq Ch^{1/2}$.

The main error analysis of the DLN-SAV method is summarized as follows.

Theorem 4 *We assume*

$$\begin{aligned} u(\cdot, t) &\in H^{s+1}(\Omega), \quad \forall t \in [0, T], \\ u &\in \ell^2_\beta(0, N; L^2(\Omega)), \quad u_t \in L^\infty(0, T; L^2(\Omega)) \cap L^2(0, T; H^{s+1}(\Omega)) \\ u_{tt} &\in L^2(0, T; H^{s+1}(\Omega)), \quad u_{ttt} \in L^2(0, T; L^2(\Omega)), \quad r_{tt} \in L^2((0, T)), \end{aligned}$$

the approximations of the DLN-SAV algorithm satisfy

$$\|e^n_u\| \leq Ch, \quad n = 0, 1, 2, \dots, M - 1, \tag{72}$$

the maximum time step has bound $k_{\max} \leq \min\{1, h^{1/2}\}$ and the time step ratios satisfy

$$C_\ell < \frac{k_n}{k_{n-1}} < C_u, \quad n = 1, 2, \dots, M - 1, \tag{73}$$

for some $C_\ell, C_u > 0$. Moreover we assume that the initial two DLN-SAV solutions u_0^h and u_1^h satisfy

$$\|u_n^h - u_n\|_1 \leq \mathcal{O}(h^s), \quad n = 0, 1. \tag{74}$$

Then we have

$$\|e_M^u\| + \|\nabla e_M^u\| \leq \mathcal{O}(k_{\max}^2, h^s), \quad M = 0, 1, \dots, N. \tag{75}$$

Proof The exact solutions of (52) satisfy

$$\begin{cases} (u_t, v^h) + \lambda(u, v) + \epsilon^2(\nabla u, \nabla v^h) + \left(\frac{r}{\sqrt{E(u)} + C_0} g(u), v^h\right) = 0, \\ r_t = \frac{1}{2\sqrt{E(u)} + C_0} \int_\Omega g(u) u_t dx, \end{cases} \quad \forall v^h \in X_s^h. \tag{76}$$

We subtract the first equation of (76) evaluated at $t_{n,\beta}$ from the first equation of DLN-SAV algorithm (53) and apply integration by parts to obtain

$$\begin{aligned} &\left(\frac{e_{n,\alpha}^u}{k_n}, v^h\right) + \epsilon^2(\nabla e_{n,\beta}^u, \nabla v^h) + \lambda(e_{n,\beta}^u, v^h) + e_{n,\beta}^r \left(\frac{g(u_{n,*}^h)}{\sqrt{E(u_{n,*}^h)} + C_0}, v^h\right) \\ &= \left(\frac{u_{n,\alpha}}{k_n} - u_t(t_{n,\beta}), v^h\right) + \epsilon^2(\nabla(u_{n,\beta} - u(t_{n,\beta})), \nabla v^h) + \lambda(u_{n,\beta} - u(t_{n,\beta}), v^h) \\ &\quad + r_{n,\beta}(\mathcal{G}_n^1, v^h) + (r_{n,\beta} - r(t_{n,\beta})) \left(\frac{g(u_{n,*})}{\sqrt{E(u_{n,*})} + C_0}, v^h\right) + r(t_{n,\beta})(\mathcal{G}_n^2, v^h), \end{aligned} \tag{77}$$

where

$$\begin{aligned} \mathcal{G}_n^1 &= \frac{g(u_{n,*}^h)}{\sqrt{E(u_{n,*}^h)} + C_0} - \frac{g(u_{n,*})}{\sqrt{E(u_{n,*})} + C_0}, \\ \mathcal{G}_n^2 &= \frac{g(u_{n,*})}{\sqrt{E(u_{n,*})} + C_0} - \frac{g(u(t_{n,\beta}))}{\sqrt{E(u(t_{n,\beta}))} + C_0}. \end{aligned} \tag{78}$$

Following the error decomposition $e_n^u = \eta_n + \phi_n^h$, Eq. (77) becomes

$$\begin{aligned} & \left(\frac{\phi_{n,\alpha}^h}{\widehat{k}_n}, v^h \right) + \epsilon^2 (\nabla \phi_{n,\beta}^h, \nabla v^h) + \lambda (\phi_{n,\beta}^h, v^h) + e_{n,\beta}^r \left(\frac{g(u_{n,*}^h)}{\sqrt{E(u_{n,*}^h) + C_0}}, v^h \right) \\ &= \left(\frac{u_{n,\alpha}}{\widehat{k}_n} - u_t(t_{n,\beta}), v^h \right) + \epsilon^2 (\nabla (u_{n,\beta} - u(t_{n,\beta})), \nabla v^h) + \lambda (u_{n,\beta} - u(t_{n,\beta}), v^h) \\ & \quad + r_{n,\beta} (\mathcal{G}_n^1, v^h) + (r_{n,\beta} - r(t_{n,\beta})) \left(\frac{g(u_{n,*})}{\sqrt{E(u_{n,*}) + C_0}}, v^h \right) + r(t_{n,\beta}) (\mathcal{G}_n^2, v^h) \\ & \quad - \left(\frac{\eta_{n,\alpha}}{\widehat{k}_n}, v^h \right) - \lambda (\eta_{n,\beta}, v^h), \end{aligned} \tag{79}$$

for $n = 1, 2, \dots, M - 1$, where the fact $\epsilon^2 (\nabla \eta_{n,\beta}, \nabla \phi_{n,\alpha}^h) = 0$ is utilized in (79), due to the definition of Ritz projection.

We subtract the second equation of (76) evaluated at $t_{n,\beta}$ from the second equation of (53) and use the notation in (78) to derive

$$\begin{aligned} \frac{e_{n,\alpha}^r}{\widehat{k}_n} &= \left(\frac{g(u_{n,*}^h)}{2\sqrt{E(u_{n,*}^h) + C_0}}, \frac{\phi_{n,\alpha}^h}{\widehat{k}_n} \right) + \left(\frac{g(u_{n,*}^h)}{2\sqrt{E(u_{n,*}^h) + C_0}}, \frac{\eta_{n,\alpha}}{\widehat{k}_n} \right) - \left(\frac{\mathcal{G}_n^1 + \mathcal{G}_n^2}{2}, \frac{u_{n,\alpha}}{\widehat{k}_n} \right) \\ & \quad + \left(\frac{g(u(t_{n,\beta}))}{2\sqrt{E(u_{n,\beta}) + C_0}}, u_t(t_{n,\beta}) - \frac{u_{n,\alpha}}{\widehat{k}_n} \right) + \left(\frac{r_{n,\alpha}}{\widehat{k}_n} - r_t(t_{n,\beta}) \right). \end{aligned} \tag{80}$$

Setting $v^h = \phi_{n,\alpha}^h$ in (79), multiplying (80) by $e_{n,\beta}^r$, adding these two equations together and utilizing the G -stability identity (7) yield

$$\begin{aligned} & \frac{1}{\widehat{k}_n} \|\phi_{n,\alpha}^h\|^2 + \epsilon^2 \left[\left\| \frac{\nabla \phi_{n+1}^h}{\nabla \phi_n^h} \right\|_{G(\theta)}^2 - \left\| \frac{\nabla \phi_n^h}{\nabla \phi_{n-1}^h} \right\|_{G(\theta)}^2 + \left\| \nabla \left(\sum_{\ell=0}^2 \gamma_\ell^{(n)} \phi_{n-1+\ell}^h \right) \right\|^2 \right] \\ & \quad + \lambda \left[\left\| \frac{\phi_{n+1}^h}{\phi_n^h} \right\|_{G(\theta)}^2 - \left\| \frac{\phi_n^h}{\phi_{n-1}^h} \right\|_{G(\theta)}^2 + \left\| \sum_{\ell=0}^2 \gamma_\ell^{(n)} \phi_{n-1+\ell}^h \right\|^2 \right] \\ & \quad + \left\| \frac{e_{n+1}^r}{e_n^r} \right\|_{G(\theta)}^2 - \left\| \frac{e_n^r}{e_{n-1}^r} \right\|_{G(\theta)}^2 + \left\| \sum_{\ell=0}^2 \gamma_\ell^{(n)} e_{n-1+\ell}^r \right\|^2 \\ &= - \left(\frac{\eta_{n,\alpha}}{\widehat{k}_n}, \phi_{n,\alpha}^h \right) - \lambda (\eta_{n,\beta}, \phi_{n,\alpha}^h) + \left(\frac{u_{n,\alpha}}{\widehat{k}_n} - u_t, \phi_{n,\alpha}^h \right) + \epsilon^2 (\Delta (u(t_{n,\beta}) - u_{n,\beta}), \phi_{n,\alpha}^h) \\ & \quad + \lambda (u_{n,\beta} - u(t_{n,\beta}), \phi_{n,\alpha}^h) + r_{n,\beta} (\mathcal{G}_n^1, \phi_{n,\alpha}^h) + (r_{n,\beta} - r(t_{n,\beta})) \left(\frac{g(u_{n,*})}{\sqrt{E(u_{n,*}) + C_0}}, \phi_{n,\alpha}^h \right) \\ & \quad + r(t_{n,\beta}) (\mathcal{G}_n^2, \phi_{n,\alpha}^h) + e_{n,\beta}^r \left(\frac{g(u_{n,*}^h)}{2\sqrt{E(u_{n,*}^h) + C_0}}, \eta_{n,\alpha} \right) - e_{n,\beta}^r \left(\frac{\mathcal{G}_n^1 + \mathcal{G}_n^2}{2}, u_{n,\alpha} \right) \\ & \quad + e_{n,\beta}^r \widehat{k}_n \left(\frac{g(u(t_{n,\beta}))}{2\sqrt{E(u_{n,\beta}) + C_0}}, u_t(t_{n,\beta}) - \frac{u_{n,\alpha}}{\widehat{k}_n} \right) + e_{n,\beta}^r \widehat{k}_n \left(\frac{r_{n,\alpha}}{\widehat{k}_n} - r_t(t_{n,\beta}) \right). \end{aligned} \tag{81}$$

Now we deal with each term on the right side of (81). By similar argument to (38)-(40)

$$- \left(\frac{\eta_{n,\alpha}}{\widehat{k}_n}, \phi_{n,\alpha}^h \right) \leq Ch^{2s+2} \int_{t_{n-1}}^{t_{n+1}} \|u_t\|_{s+1}^2 dt + \frac{\|\phi_{n,\alpha}^h\|^2}{8\widehat{k}_n}. \tag{82}$$

By the approximation theorem in (32), triangle inequality and Lemma 3

$$\begin{aligned}
 -\lambda(\eta_{n,\beta}, \phi_{n,\alpha}^h) &\leq Ch^{2s+2}\widehat{k}_n\|u_{n,\beta}\|_{s+1}^2 + \frac{\|\phi_{n,\alpha}^h\|^2}{8\widehat{k}_n} \\
 &\leq Ch^{2s+2}\widehat{k}_n(\|u_{n,\beta} - u(t_{n,\beta})\|_{s+1}^2 + \|u(t_{n,\beta})\|_{s+1}^2) + \frac{\|\phi_{n,\alpha}^h\|^2}{8\widehat{k}_n} \\
 &\leq Ch^{2s+2}\left(k_{\max}^4\int_{t_{n-1}}^{t_{n+1}}\|u_{tt}\|_{s+1}^2 dt + (k_n+k_{n-1})\|u(t_{n,\beta})\|_{s+1}^2\right) + \frac{\|\phi_{n,\alpha}^h\|^2}{8\widehat{k}_n}. \tag{83}
 \end{aligned}$$

By Cauchy-Schwarz inequality, Young’s inequality and Lemma 3

$$\begin{aligned}
 \left(u_t - \frac{u_{n,\alpha}}{\widehat{k}_n}, \phi_{n,\alpha}^h\right) &\leq C\widehat{k}_n\left\|\frac{u_{n,\alpha}}{\widehat{k}_n} - u_t\right\|^2 + \frac{\|\phi_{n,\alpha}^h\|^2}{8\widehat{k}_n} \\
 &\leq Ck_{\max}^4\int_{t_{n-1}}^{t_{n+1}}\|u_{ttt}\|^2 dt + \frac{\|\phi_{n,\alpha}^h\|^2}{8\widehat{k}_n}, \tag{84}
 \end{aligned}$$

$$\begin{aligned}
 \epsilon^2\left(\Delta(u_{n,\beta} - u(t_{n,\beta})), \phi_{n,\alpha}^h\right) &\leq \epsilon^2\widehat{k}_n\|\Delta(u_{n,\beta} - u(t_{n,\beta}))\|^2 + \frac{\|\phi_{n,\alpha}^h\|^2}{8\widehat{k}_n} \\
 &\leq Ck_{\max}^4\int_{t_{n-1}}^{t_{n+1}}\|\Delta u_{tt}\|^2 dt + \frac{\|\phi_{n,\alpha}^h\|^2}{8\widehat{k}_n}, \tag{85}
 \end{aligned}$$

$$\begin{aligned}
 \lambda(u_{n,\beta} - u(t_{n,\beta}), \phi_{n,\alpha}^h) &\leq \lambda\widehat{k}_n\|u_{n,\beta} - u(t_{n,\beta})\|^2 + \frac{\|\phi_{n,\alpha}^h\|^2}{8\widehat{k}_n} \\
 &\leq Ck_{\max}^4\int_{t_{n-1}}^{t_{n+1}}\|u_{tt}\|^2 dt + \frac{\|\phi_{n,\alpha}^h\|^2}{8\widehat{k}_n}. \tag{86}
 \end{aligned}$$

By algebraic calculation, $\mathcal{G}_n^1 = \mathcal{G}_n^{11} + \mathcal{G}_n^{12}$, where

$$\begin{aligned}
 \mathcal{G}_n^{11} &= \frac{g(u_{n,*}^h) - g(u_{n,*})}{\sqrt{E(u_{n,*}^h) + C_0}}, \\
 \mathcal{G}_n^{12} &= \frac{g(u_{n,*})(E(u_{n,*}) - E(u_{n,*}^h))}{\sqrt{E(u_{n,*}) + C_0}\sqrt{E(u_{n,*}^h) + C_0}(\sqrt{E(u_{n,*}) + C_0} + \sqrt{E(u_{n,*}^h) + C_0})}. \tag{87}
 \end{aligned}$$

By maximum principle of exact solutions, we have that $r(t)$ is uniformly bounded for all t , $\{\|u_{n,*}\|_{\infty}\}_{n=1}^{M-1}$ is uniformly bounded and $\sqrt{E(u_{n,*}) + C_0} > C_r$ for $1 \leq n \leq M - 1$. Meanwhile by assumption, we have $\{\|u_{n,*}^h\|_{\infty}\}_{n=1}^{M-1}$ is uniformly bounded and $\sqrt{E(u_{n,*}^h) + C_0} > C_r/2$ for $1 \leq n \leq M - 1$. Thus

$$\begin{aligned}
 r_{n,\beta}(\mathcal{G}_n^{11}, \phi_{n,\alpha}^h) &\leq |r_{n,\beta}| \int_{\Omega} \frac{|g(u_{n,*}^h) - g(u_{n,*})|\phi_{n,\alpha}^h}{\sqrt{E(u_{n,*}^h) + C_0}} dx \\
 &\leq C \int_{\Omega} |u_{n,*}^h - u_{n,*}|(u_{n,*}^h)^2 + u_{n,*}^2 + u_{n,*}^h u_{n,*} - 1 - \lambda|\phi_{n,\alpha}^h| dx \\
 &\leq C \int_{\Omega} (|\phi_{n,*}^h| + |\eta_{n,*}|)|\phi_{n,\alpha}^h| dx \\
 &\leq C\widehat{k}_n(\|\phi_n^h\|^2 + \|\phi_{n-1}^h\|^2) + C\widehat{k}_n\|\eta_{n,*}\|^2 + \frac{\|\phi_{n,\alpha}^h\|^2}{16\widehat{k}_n}. \tag{88}
 \end{aligned}$$

We apply approximation theorem (32), triangle inequality, Lemma 3 to (88)

$$\begin{aligned}
 r_{n,\beta}(\mathcal{G}_n^{11}, \phi_{n,\alpha}^h) &\leq C\widehat{k}_n(\|\phi_n^h\|^2 + \|\phi_{n-1}^h\|^2) + Ch^{2s+2}\widehat{k}_n(\|u_{n,*} - u(t_{n,\beta})\|_{s+1}^2 + \|u(t_{n,\beta})\|_{s+1}^2) + \frac{\|\phi_{n,\alpha}^h\|^2}{16\widehat{k}_n} \\
 &\leq C\widehat{k}_n(\|\phi_n^h\|^2 + \|\phi_{n-1}^h\|^2) + \frac{\|\phi_{n,\alpha}^h\|^2}{16\widehat{k}_n} \\
 &\quad + Ch^{2s+2}\left(k_{\max}^4 \int_{t_{n-1}}^{t_{n+1}} \|u_{tt}\|_{s+1}^2 dt + (k_n + k_{n-1})\|u(t_{n,\beta})\|_{s+1}^2\right), \tag{89}
 \end{aligned}$$

where $u_{n,*}$ is the second-order approximation to $u(t_{n,\beta})$ in time is used in the last inequality. Similarly,

$$\begin{aligned}
 r_{n,\beta}(\mathcal{G}_n^{12}, \phi_{n,\alpha}^h) &\leq C|E(u_{n,*}) - E(u_{n,*}^h)| \int_{\Omega} |\phi_{n,\alpha}^h| dx \\
 &\leq C \int_{\Omega} |u_{n,*} - u_{n,*}^h| |u_{n,*} + u_{n,*}^h| \left| \frac{1}{4}(u_{n,*}^2 + (u_{n,*}^h)^2) - \frac{1+\lambda}{2} \right| dx \int_{\Omega} |\phi_{n,\alpha}^h| dx \\
 &\leq C(\|\phi_{n,*}^h\| + \|\eta_{n,*}\|) \|\phi_{n,\alpha}^h\| \\
 &\leq C\widehat{k}_n(\|\phi_n^h\|^2 + \|\phi_{n-1}^h\|^2) + C\widehat{k}_n\|\eta_{n,*}\|^2 + \frac{\|\phi_{n,\alpha}^h\|^2}{16\widehat{k}_n} \\
 &\leq C\widehat{k}_n(\|\phi_n^h\|^2 + \|\phi_{n-1}^h\|^2) + \frac{\|\phi_{n,\alpha}^h\|^2}{16\widehat{k}_n} \\
 &\quad + Ch^{2s+2}\left(k_{\max}^4 \int_{t_{n-1}}^{t_{n+1}} \|u_{tt}\|_{s+1}^2 dt + (k_n + k_{n-1})\|u(t_{n,\beta})\|_{s+1}^2\right). \tag{90}
 \end{aligned}$$

We combine (89) and (90) to obtain

$$\begin{aligned}
 r_{n,\beta}(\mathcal{G}_n^1, \phi_{n,\alpha}^h) &\leq C\widehat{k}_n(\|\phi_n^h\|^2 + \|\phi_{n-1}^h\|^2) + \frac{\|\phi_{n,\alpha}^h\|^2}{8\widehat{k}_n} \\
 &\quad + Ch^{2s+2}\left(k_{\max}^4 \int_{t_{n-1}}^{t_{n+1}} \|u_{tt}\|_{s+1}^2 dt + (k_n + k_{n-1})\|u(t_{n,\beta})\|_{s+1}^2\right). \tag{91}
 \end{aligned}$$

By the uniform boundedness of $r(t)$, $\|u(t)\|_{\infty}$ for all t , Cauchy-Schwarz inequality and Lemma 3

$$\begin{aligned}
 (r_{n,\beta} - r(t_{n,\beta}))\left(\frac{g(u_{n,*})}{\sqrt{E(u_{n,*})} + C_0}, \phi_{n,\alpha}^h\right) &\leq C\widehat{k}_n|r_{n,\beta} - r(t_{n,\beta})|^2 + \frac{\|\phi_{n,\alpha}^h\|^2}{8\widehat{k}_n} \\
 &\leq Ck_{\max}^4 \int_{t_{n-1}}^{t_{n+1}} |r_{tt}|^2 dt + \frac{\|\phi_{n,\alpha}^h\|^2}{8\widehat{k}_n}. \tag{92}
 \end{aligned}$$

Similar to (89)-(92)

$$r(t_{n,\beta})(\mathcal{G}_n^2, \phi_{n,\alpha}^h) \leq Ck_{\max}^4 \int_{t_{n-1}}^{t_{n+1}} \|u_{tt}\|^2 dt + \frac{\|\phi_{n,\alpha}^h\|^2}{8\widehat{k}_n}. \tag{93}$$

By the assumption in (72), $\{\|u_{n,*}^h\|_{\infty}\}_{n=1}^{M-1}$ is uniformly bounded and

$\sqrt{E(u_{n,*}^h) + C_0} > C_r/2$ for $1 \leq n \leq M - 1$. Thus

$$\begin{aligned}
 & e_{n,\beta}^r \left(\frac{g(u_{n,*}^h)}{2\sqrt{E(u_{n,*}^h) + C_0}}, \eta_{n,\alpha} \right) \\
 & \leq Ch^{s+1} |e_{n,\beta}^r| \|\alpha_2(u_{n+1} - u_n) + \alpha_0(u_n - u_{n-1})\|_{s+1} \\
 & \leq C(\theta)h^{s+1} |e_{n,\beta}^r| (\|u_{n+1} - u_n\|_{s+1} + \|u_n - u_{n-1}\|_{s+1}) \\
 & \leq C(\theta)h^{s+1} |e_{n,\beta}^r| \left[\left(k_n \int_{t_n}^{t_{n+1}} \|u_t\|_{s+1}^2 dt \right)^{1/2} + \left(k_{n-1} \int_{t_{n-1}}^{t_n} \|u_t\|_{s+1}^2 dt \right)^{1/2} \right] \\
 & \leq C(\theta)(k_n + k_{n-1})^{1/2} h^{s+1} |e_{n,\beta}^r| \left(\int_{t_{n-1}}^{t_{n+1}} \|u_t\|_{s+1}^2 dt \right)^{1/2} \\
 & \leq \frac{\delta}{4} (k_n + k_{n-1}) |e_{n,\beta}^r|^2 + C(\theta, \delta) h^{2s+2} \int_{t_{n-1}}^{t_{n+1}} \|u_t\|_{s+1}^2 dt, \tag{94}
 \end{aligned}$$

where $\delta > 0$ is a certain constant to be decided later. We use the assumption in (72) again and the approximation theorem (32) to obtain

$$\begin{aligned}
 & \frac{1}{2} e_{n,\beta}^r \left(\mathcal{G}_n^1, u_{n,\alpha} \right) \\
 & \leq C |e_{n,\beta}^r| \left(\int_{\Omega} |u_{n,*}^h - u_{n,*}| |u_{n,\alpha}| dx + \int_{\Omega} |u_{n,*}^h - u_{n,*}| dx \int_{\Omega} |u_{n,\alpha}| dx \right) \\
 & \leq C(\theta) |e_{n,\beta}^r| (\|\eta_{n,*}\| + \|\phi_{n,*}^h\|) (\|u_{n+1} - u_n\| + \|u_n - u_{n-1}\|) \\
 & \leq C(\theta)(k_n + k_{n-1})^{1/2} |e_{n,\beta}^r| (Ch^{s+1} \|u_{n,*}\|_{s+1} + \|\phi_{n,*}^h\|) \left(\int_{t_{n-1}}^{t_{n+1}} \|u_t\|^2 dt \right)^{1/2} \\
 & \leq C(\theta)(k_n + k_{n-1}) |e_{n,\beta}^r| \|u_t\|_{L^\infty(0,T;L^2(\Omega))} (Ch^{s+1} \|u_{n,*}\|_{s+1} + \|\phi_{n,*}^h\|) \tag{95}
 \end{aligned}$$

By triangle inequality, Young’s inequality and the fact that $u_{n,*}$ is the second-order approximation to $u(t_n, \beta)$ in time

$$\begin{aligned}
 & C(\theta)(k_n + k_{n-1})h^{s+1} |e_{n,\beta}^r| \|u_t\|_{L^\infty(0,T;L^2(\Omega))} \|u_{n,*}\|_{s+1} \\
 & \leq C(\theta, \delta)(k_n + k_{n-1})h^{2s+2} \|u_t\|_{L^\infty(0,T;L^2(\Omega))}^2 (\|u_{n,*} - u(t_n, \beta)\|_{s+1}^2 + \|u(t_n, \beta)\|_{s+1}^2) \\
 & \quad + \frac{\delta}{16} (k_n + k_{n-1}) |e_{n,\beta}^r|^2 \\
 & \leq C(\theta, \delta)h^{2s+2} \|u_t\|_{L^\infty(0,T;L^2(\Omega))}^2 \left(k_{\max}^4 \int_{t_{n-1}}^{t_{n+1}} \|u_{tt}\|_{s+1}^2 dt + (k_n + k_{n-1}) \|u(t_n, \beta)\|_{s+1}^2 \right) \\
 & \quad + \frac{\delta}{16} (k_n + k_{n-1}) |e_{n,\beta}^r|^2. \tag{96}
 \end{aligned}$$

$$\begin{aligned}
 & C(\theta)(k_n + k_{n-1}) |e_{n,\beta}^r| \|u_t\|_{L^\infty(0,T;L^2(\Omega))} \|\phi_{n,*}^h\| \\
 & \leq \frac{\delta}{16} (k_n + k_{n-1}) |e_{n,\beta}^r|^2 + C(\theta, \delta)(k_n + k_{n-1}) \|u_t\|_{L^\infty(0,T;L^2(\Omega))}^2 (\|\phi_n^h\|^2 + \|\phi_{n-1}^h\|^2). \tag{97}
 \end{aligned}$$

We combine (95), (96), (97) to have

$$\frac{1}{2} e_{n,\beta}^r \left(\mathcal{G}_n^1, u_{n,\alpha} \right)$$

$$\begin{aligned} &\leq C(\theta, \delta)h^{2s+2}\|u_t\|_{L^\infty(0,T;L^2(\Omega))}^2 \left(k_{\max}^4 \int_{t_{n-1}}^{t_{n+1}} \|u_{tt}\|_{s+1}^2 dt + (k_n + k_{n-1})\|u(t_n, \beta)\|_{s+1}^2 \right) \\ &\quad + C(\theta, \delta)(k_n + k_{n-1})\|u_t\|_{L^\infty(0,T;L^2(\Omega))}^2 (\|\phi_n^h\|^2 + \|\phi_{n-1}^h\|^2) + \frac{\delta}{8}(k_n + k_{n-1})|e_{n,\beta}^r|^2. \end{aligned} \tag{98}$$

By the maximum bound principle for the exact solution and Hölder’s inequality

$$\begin{aligned} &\frac{1}{2}e_{n,\beta}^r \left(\mathcal{G}_n^2, u_{n,\alpha} \right) \\ &\leq C|e_{n,\beta}^r| \left(\int_{\Omega} |u_{n,*} - u(t_n, \beta)| |u_{n,\alpha}| dx + \int_{\Omega} |u_{n,*} - u(t_n, \beta)| dx \int_{\Omega} |u_{n,\alpha}| dx \right) \\ &\leq C(\theta)|e_{n,\beta}^r| \|u_{n,*} - u(t_n, \beta)\| (\|u_{n+1} - u_n\| + \|u_n - u_{n-1}\|) \\ &\leq C(\theta)|e_{n,\beta}^r| \|u_{n,*} - u(t_n, \beta)\| \left[\left(k_n \int_{t_n}^{t_{n+1}} \|u_t(t)\|^2 dt \right)^{\frac{1}{2}} + \left(k_{n-1} \int_{t_{n-1}}^{t_n} \|u_t(t)\|^2 dt \right)^{\frac{1}{2}} \right] \\ &\leq C(\theta)(k_n + k_{n-1})\|u_t\|_{L^\infty(0,T;L^2(\Omega))} |e_{n,\beta}^r| \|u_{n,*} - u(t_n, \beta)\| \\ &\leq \frac{\delta}{8}(k_n + k_{n-1})|e_{n,\beta}^r|^2 + C(\theta, \delta)\|u_t\|_{L^\infty(0,T;L^2(\Omega))}^2 k_{\max}^4 \int_{t_{n-1}}^{t_{n+1}} \|u_{tt}\|^2 dt. \end{aligned} \tag{99}$$

By the maximum bound principle for the exact solution and Lemma 3

$$\begin{aligned} &e_{n,\beta}^r \widehat{k}_n \left(\frac{g(u(t_n, \beta))}{2\sqrt{E(u_n, \beta)} + C_0}, u_t(t_n, \beta) - \frac{u_{n,\alpha}}{\widehat{k}_n} \right) \\ &\leq C\widehat{k}_n |e_{n,\beta}^r| \left\| u_t(t_n, \beta) - \frac{u_{n,\alpha}}{\widehat{k}_n} \right\| \\ &\leq \frac{\delta}{4}(k_n + k_{n-1})|e_{n,\beta}^r|^2 + C(\theta, \delta)k_{\max}^4 \int_{t_{n-1}}^{t_{n+1}} \|u_{tt}\|^2 dt. \end{aligned} \tag{100}$$

$$e_{n,\beta}^r \widehat{k}_n \left(\frac{r_{n,\alpha}}{\widehat{k}_n} - r_t(t_n, \beta) \right) \leq \frac{\delta}{4}(k_n + k_{n-1})|e_{n,\beta}^r|^2 + C(\delta)k_{\max}^4 \int_{t_{n-1}}^{t_{n+1}} |r_{tt}|^2 dt. \tag{101}$$

We combine (81) - (86), (91) - (94), (98) - (101) and drop the numerical dissipation terms

$$\begin{aligned} &\epsilon^2 \left[\left\| \frac{\nabla \phi_{n+1}^h}{\nabla \phi_n^h} \right\|_{G(\theta)}^2 - \left\| \frac{\nabla \phi_n^h}{\nabla \phi_{n-1}^h} \right\|_{G(\theta)}^2 \right] + \lambda \left[\left\| \frac{\phi_{n+1}^h}{\phi_n^h} \right\|_{G(\theta)}^2 - \left\| \frac{\phi_n^h}{\phi_{n-1}^h} \right\|_{G(\theta)}^2 \right] \\ &\quad + \left\| \frac{e_{n+1}^r}{e_n^r} \right\|_{G(\theta)}^2 - \left\| \frac{e_n^r}{e_{n-1}^r} \right\|_{G(\theta)}^2 \\ &\leq C\widehat{k}_n (\|\phi_n^h\|^2 + \|\phi_{n-1}^h\|^2) + C(\theta, \delta)(k_n + k_{n-1})\|u_t\|_{L^\infty(0,T;L^2(\Omega))}^2 (\|\phi_n^h\|^2 + \|\phi_{n-1}^h\|^2) \\ &\quad + \delta(k_n + k_{n-1})|e_{n,\beta}^r|^2 + C(\theta, \delta)h^{2s+2} \int_{t_{n-1}}^{t_{n+1}} \|u_t\|_{s+1}^2 dt \\ &\quad + Ch^{2s+2} \left(k_{\max}^4 \int_{t_{n-1}}^{t_{n+1}} \|u_{tt}\|_{s+1}^2 dt + (k_n + k_{n-1})\|u(t_n, \beta)\|_{s+1}^2 \right) \\ &\quad + Ck_{\max}^4 \int_{t_{n-1}}^{t_{n+1}} \|u_{ttt}\|^2 dt + Ck_{\max}^4 \int_{t_{n-1}}^{t_{n+1}} \|\Delta u_{tt}\|^2 dt + C(\delta)k_{\max}^4 \int_{t_{n-1}}^{t_{n+1}} |r_{tt}|^2 dt \\ &\quad + C(\theta, \delta)h^{2s+2}\|u_t\|_{L^\infty(0,T;L^2(\Omega))}^2 \left(k_{\max}^4 \int_{t_{n-1}}^{t_{n+1}} \|u_{tt}\|_{s+1}^2 dt + (k_n + k_{n-1})\|u(t_n, \beta)\|_{s+1}^2 \right) \end{aligned}$$

$$+ C(\theta, \delta)(\|u_t\|_{L^\infty(0,T;L^2(\Omega))}^2 + 1)k_{\max}^4 \int_{t_{n-1}}^{t_{n+1}} \|u_{tt}\|^2 dt. \tag{102}$$

We sum (102) over n from 1 to $N - 1$ and use time step ratio bounds in (73)

$$\begin{aligned} & \epsilon^2 \left(\frac{1+\theta}{4} \|\nabla \phi_N^h\|^2 + \frac{1-\theta}{4} \|\nabla \phi_{N-1}^h\|^2 \right) + \lambda \left(\frac{1+\theta}{4} \|\phi_N^h\|^2 + \frac{1-\theta}{4} \|\phi_{N-1}^h\|^2 \right) \\ & + \left(\frac{1+\theta}{4} \|e_N^r\|^2 + \frac{1-\theta}{4} \|e_{N-1}^r\|^2 \right) \\ & \leq \sum_{n=0}^{N-1} C(\theta, \delta)k_n(\|u_t\|_{L^\infty(0,T;L^2(\Omega))}^2 + 1)\|\phi_n^h\|^2 + 3\delta C_\beta^2(\theta)k_{N-1}|e_n|^2 \\ & + 9\delta C_\beta^2(\theta) \sum_{n=0}^{N-1} k_n |e_n^r|^2 + C(\theta, \delta)h^{2s+2}\|u_t\|_{L^2(0,T;H^{s+1})}^2 + Ch^{2s+2}\|u\|_{e_\beta^2(0,N;H^{s+1})}^2 \\ & + Ch^{2s+2}k_{\max}^4\|u_{tt}\|_{L^2(0,T;H^{s+1})}^2 + Ck_{\max}^4(\|u_{ttt}\|_{L^2(0,T,L^2)}^2 + \|\Delta u_{tt}\|_{L^2(0,T,L^2)}^2) \\ & + C(\delta)k_{\max}^4 \int_0^T |r_{tt}|^2 dt + C(\theta, \delta)k_{\max}^4(1 + \|u_t\|_{L^\infty(0,T;L^2(\Omega))}^2)\|u_{tt}\|_{L^2(0,T;L^2)}^2 \\ & + C(\theta, \delta)h^{2s+2}\|u_{tt}\|_{L^\infty(0,T;L^2(\Omega))}^2 \left(k_{\max}^4\|u_{tt}\|_{L^2(0,T;H^{s+1})}^2 + \|u\|_{e_\beta^2(0,N;H^{s+1})}^2 \right) \\ & + \epsilon^2 \left(\frac{1+\theta}{4} \|\nabla \phi_1^h\|^2 + \frac{1-\theta}{4} \|\nabla \phi_0^h\|^2 \right) + \lambda \left(\frac{1+\theta}{4} \|\phi_1^h\|^2 + \frac{1-\theta}{4} \|\phi_0^h\|^2 \right) \\ & + \left(\frac{1+\theta}{4} |e_1^r|^2 + \frac{1-\theta}{4} |e_0^r|^2 \right). \tag{103} \end{aligned}$$

We set $\delta = (1 + \theta)/(12C_\beta^2(\theta))$ and apply the discrete Grönwall inequality [23] with the time step restriction $k_{\max} < 1$ to (103)

$$\begin{aligned} & \frac{\epsilon\sqrt{1+\theta}}{2} \|\nabla \phi_N^h\| + \frac{\sqrt{\lambda(1+\theta)}}{2} \|\phi_N^h\| \\ & \leq C(T, \theta, \|u_t\|_{L^\infty(0,T;L^2(\Omega))}) \left\{ h^{s+1}\|u_t\|_{L^2(0,T;H^{s+1})} + h^{s+1}\|u\|_{e_\beta^2(0,N;H^{s+1})} \right. \\ & + Ch^{s+1}k_{\max}^2\|u_{tt}\|_{L^2(0,T;H^{s+1})} + k_{\max}^2(\|u_{ttt}\|_{L^2(0,T,L^2)} + \|\Delta u_{tt}\|_{L^2(0,T,L^2)}) \\ & + k_{\max}^2\|r_{tt}\|_{L^2(0,T)} + k_{\max}^2(1 + \|u_t\|_{L^\infty(0,T;L^2(\Omega))})\|u_{tt}\|_{L^2(0,T;L^2)} \\ & + h^{s+1}\|u_t\|_{L^\infty(0,T;L^2(\Omega))} \left(k_{\max}^2\|u_{tt}\|_{L^2(0,T;H^{s+1})} + \|u\|_{e_\beta^2(0,N;H^{s+1})} \right) \\ & + \frac{\epsilon\sqrt{1+\theta}}{2} \|\nabla \phi_1^h\| + \frac{\epsilon\sqrt{1-\theta}}{2} \|\nabla \phi_0^h\| + \frac{\sqrt{\lambda(1+\theta)}}{2} \|\phi_1^h\| + \frac{\sqrt{\lambda(1-\theta)}}{2} \|\phi_0^h\| \\ & \left. + \frac{\sqrt{1+\theta}}{2} |e_1^r| + \frac{\sqrt{1-\theta}}{2} |e_0^r| \right\}. \tag{104} \end{aligned}$$

We use the triangle inequality, approximation theorem in (32), (104) and initial conditions in (74) to have (75). □

Remark 8 From (104), we can conclude that $\|e_M^u\| \leq \mathcal{O}(k_{\max}^2, h^{s+1})$ achieves the optimal error estimate in the L^2 norm, if the initial two step solutions match the exact solutions (leading to zero ϕ_0^h and ϕ_1^h). This is also verified by Table 4 in the one-dimensional traveling wave test problem in Subsection 6.1.

5 Time Adaptivity

In this section, we discuss adaptive DLN algorithms for solving the Allen-Cahn equation, to better take advantage of this variable time-stepping method. Here we consider adaptive DLN algorithms by using the LTE criterion, which involve two essential parts:

- the estimator for LTE,
- the time step controller.

An explicit, variable step AB2-like scheme¹The deviation of this scheme is similar to two-step Adam-Bashforth scheme, thus we name it an AB2-like scheme. is adopted to estimate the LTE of the DLN method. The AB2-like time-stepping scheme, applying to the initial value problem in (3), takes the form

$$y_{n+1}^{AB2-like} = y_n + \frac{t_{n+1} - t_n}{2(t_{n-1,\beta} - t_{n-2,\beta})} \left[(t_{n+1} + t_n - 2t_{n-2,\beta})g^{DLN}(t_{n-1,\beta}, y_{n-1,\beta}) - (t_{n+1} + t_n - 2t_{n-1,\beta})g^{DLN}(t_{n-2,\beta}, y_{n-2,\beta}) \right], \tag{105}$$

where $g^{DLN}(t_{n-1,\beta}, y_{n-1,\beta})$ and $g^{DLN}(t_{n-2,\beta}, y_{n-2,\beta})$ are calculated by the DLN scheme in (DLN)

$$g^{DLN}(t_{n-1,\beta}, y_{n-1,\beta}) = \frac{y_{n-1,\alpha}}{k_{n-1}}, \quad g^{DLN}(t_{n-2,\beta}, y_{n-2,\beta}) = \frac{y_{n-2,\alpha}}{k_{n-2}}.$$

Thus the AB2-like solution $y_{n+1}^{AB2-like}$ in (105) is just the linear combination of the previous four DLN solutions $\{y_n, y_{n-1}, y_{n-2}, y_{n-3}\}$, and thus obtained with low computational costs.

We denote time step ratio $\tau_n = k_n/k_{n-1}$ and utilize the AB2-like scheme (105) to estimate the LTE of the DLN method via

$$\widehat{T}_{n+1} = \frac{-G^{(n)}}{G^{(n)} + \mathcal{R}^{(n)}} (y_{n+1}^{DLN} - y_{n+1}^{AB2-like}), \tag{106}$$

where $G^{(n)}, \mathcal{R}^{(n)}$ are coefficients before the LTEs of the DLN scheme and AB2-like scheme respectively:

$$G^{(n)} = \left(\frac{1}{2} - \frac{\alpha_0}{2\alpha_2} \frac{1}{\tau_n} \right) \left(\beta_2^{(n)} - \beta_0^{(n)} \frac{1}{\tau_n} \right)^2 + \frac{\alpha_0}{6\alpha_2} \left(\frac{1}{\tau_n} \right)^3 - \frac{1}{6},$$

$$\mathcal{R}^{(n)} = \frac{1}{12} \left[2 + \frac{3}{\tau_n} \left(1 + (1 - \beta_2^{(n-2)}) \frac{1}{\tau_{n-1}} + \beta_0^{(n-2)} \frac{1}{\tau_{n-2}} \frac{1}{\tau_{n-1}} \right) \left(1 + (1 - \beta_2^{(n-1)}) \frac{1}{\tau_n} + \beta_0^{(n-1)} \frac{1}{\tau_{n-1}} \frac{1}{\tau_n} \right) + \frac{3}{\tau_n} \left(1 + \frac{1}{\tau_n} + (1 - \beta_2^{(n-2)}) \frac{1}{\tau_{n-1}} \frac{1}{\tau_n} + \beta_0^{(n-2)} \frac{1}{\tau_{n-2}} \frac{1}{\tau_{n-1}} \frac{1}{\tau_n} \right) \left(1 - \beta_2^{(n-1)} + \beta_0^{(n-1)} \frac{1}{\tau_{n-1}} \right) \right]. \tag{107}$$

We refer to [29] for the derivation of the explicit AB2-like scheme in (105) and the estimator of LTE in (106).

For the time step controller, there are many choices and we consider the following one proposed in [20]

$$k_{n+1} = k_n \cdot \min \left\{ 1.5, \max \left\{ 0.2, \kappa \left(\text{Tol} / \|\widehat{T}_{n+1}\| \right)^{\frac{1}{3}} \right\} \right\}, \tag{108}$$

where $\kappa \in (0, 1]$ is the safety factor and Tol is the required tolerance for the LTE. We summarize the adaptive DLN algorithm using the estimator of LTE in (106) and the step controller in (108) in the following pseudocode.

Algorithm 1: Adaptive DLN method (LTE estimator by AB2-like scheme)

Input: tolerance Tol, four previous DLN solutions $u_n^h, u_{n-1}^h, u_{n-2}^h, u_{n-3}^h$, current time step k_n , three previous time step $k_{n-1}, k_{n-2}, k_{n-3}$, safety factor κ ;

Compute the DLN solution $u_{n+1}^{h, \text{DLN}}$ by (19) or (53) ;

Compute the AB2-like solution $u_{n+1}^{h, \text{AB2-like}}$ by (105) ;

Use $k_n, k_{n-1}, k_{n-2}, k_{n-3}$ to update $\tau_n, \tau_{n-1}, \tau_{n-2}$;

Compute $G^{(n)}, \mathcal{R}^{(n)}$ by (107) ;

$\widehat{T}_{n+1} \leftarrow \frac{|G^{(n)}|}{|G^{(n)} + \mathcal{R}^{(n)}|} \|u_{n+1}^{h, \text{DLN}} - u_{n+1}^{h, \text{AB2-like}}\|$; // absolute estimator

or $\widehat{T}_{n+1} \leftarrow \frac{|G^{(n)}|}{|G^{(n)} + \mathcal{R}^{(n)}|} \frac{\|u_{n+1}^{h, \text{DLN}} - u_{n+1}^{h, \text{AB2-like}}\|}{\|u_{n+1}^{h, \text{DLN}}\|}$; // relative estimator

if $\widehat{T}_{n+1} < \text{Tol}$ **then**

$u_{n+1}^h \leftarrow u_{n+1}^{h, \text{DLN}}$; // accept the result

$k_{n+1} \leftarrow k_n \cdot \min \{1.5, \max \{0.2, \kappa (\frac{\text{Tol}}{\widehat{T}_{n+1}})^{1/3}\}\}$; // adjust step by (108)

else

 // adjust current step to recompute $k_n \leftarrow k_n \cdot \min \{1.5, \max \{0.2, \kappa (\frac{\text{Tol}}{\widehat{T}_{n+1}})^{1/3}\}\}$

 ;

6 Numerical Tests

In this section, we test the performance of the proposed modified DLN algorithm and DLN-SAV algorithm on three numerical tests:

- Accuracy test on the 1D traveling wave solution;
- Accuracy test on the 2D test with known solutions;
- Simulation of the 2D test with random initial conditions.

We implement these algorithms with three different values of θ : $2/3, 2/\sqrt{5}, 1$. Among these values, $\theta = 2/3$ is proposed in [11] to balance the magnitude of LTE and keep fine stability properties. The value $\theta = 2/\sqrt{5}$ is suggested in [26] to have the best stability at infinity. The algorithm with value $\theta = 1$ reduces to the classical one-step midpoint rule. In the implementation, we use MATLAB for the 1D test problem and the software FreeFem++ [22] for two 2D test problems. For the modified DLN algorithm (19), we use fixed point iteration to solve the non-linear system at each time step.

6.1 One-dimensional Traveling Wave Solution

We use the 1D traveling wave problem [5] with the known solution to test the accuracy of modified DLN and DLN-SAV algorithms. One traveling wave solution of Allen-Cahn equation (1) in 1D takes the form

$$u(x, t) = \frac{1}{2} \left[1 - \tanh \left(\frac{x - st}{2\sqrt{2}\epsilon} \right) \right], \quad -2 \leq x \leq 4,$$

where the traveling speed is $s = 3\epsilon/\sqrt{2}$. We set the final time as $T = 2$, the model parameter as $\epsilon = 0.01$, and use the inhomogeneous Dirichlet boundary condition. We use \mathbb{P}^2 finite element space in the spatial discretization.

Table 1 L^2 -norm of error and rate for 1D modified DLN scheme in time ($h = k^2$)

	k	$\ u - u^h\ _{\ell^\infty(L^2)}$	R	$\ u - u^h\ _{\ell^2(L^2)}$	R	$\ u - u^h\ _{\ell^2(H^1)}$	R
$\theta = \frac{2}{3}$	0.04	1.84e-5	-	1.56e-5	-	1.05e-3	-
	0.02	4.64e-6	1.98	3.92e-6	1.99	1.58e-4	2.73
	0.01	1.17e-6	1.99	9.82e-7	2.00	3.74e-5	2.08
	0.005	2.92e-7	2.00	2.46e-7	2.00	9.30e-6	2.01
$\theta = \frac{2}{\sqrt{5}}$	0.04	1.45e-5	-	1.14e-5	-	9.38e-4	-
	0.02	3.68e-6	1.98	2.88e-6	1.99	1.05e-4	3.16
	0.01	9.27e-7	1.99	7.23e-7	1.99	2.27e-5	2.21
	0.005	2.32e-7	2.00	1.81e-7	2.00	5.61e-6	2.02
$\theta = 1$	0.04	1.27e-5	-	9.58e-6	-	9.19e-4	-
	0.02	3.22e-6	1.98	2.42e-6	1.99	9.45e-5	3.28
	0.01	8.12e-7	1.99	6.07e-7	2.00	1.97e-5	2.26
	0.005	2.04e-7	1.99	1.52e-7	2.00	4.86e-6	2.02

Table 2 L^2 -norm of error and rate for 1D modified DLN scheme in space ($k = h^2$)

	h	$\ u - u^h\ _{\ell^\infty(L^2)}$	R	$\ u - u^h\ _{\ell^2(L^2)}$	R	$\ u - u^h\ _{\ell^2(H^1)}$	R
$\theta = \frac{2}{3}$	0.04	2.17e-3	-	2.41e-3	-	4.80e-1	-
	0.02	2.91e-4	2.90	3.97e-4	2.60	1.32e-1	1.86
	0.01	3.69e-5	2.98	5.19e-5	2.94	3.39e-2	1.97
	0.005	4.65e-6	2.99	6.57e-6	2.98	8.53e-3	1.99
$\theta = \frac{2}{\sqrt{5}}$	0.04	2.17e-3	-	2.41e-3	-	4.80e-1	-
	0.02	2.91e-4	2.90	3.97e-4	2.60	1.32e-1	1.86
	0.01	3.69e-5	2.98	5.19e-5	2.94	3.39e-2	1.97
	0.005	4.65e-6	2.99	6.57e-6	2.98	8.53e-3	1.99
$\theta = 1$	0.04	2.17e-3	-	2.41e-3	-	4.80e-1	-
	0.02	2.91e-4	2.90	3.97e-4	2.60	1.32e-1	1.86
	0.01	3.69e-5	2.98	5.19e-5	2.94	3.39e-2	1.97
	0.005	4.65e-6	2.99	6.57e-6	2.98	8.53e-3	1.99

6.1.1 Constant Time Step

First, we consider the constant time step k and set $h = k^2$ to check the accuracy of both algorithms in time. From Tables 1 and 3, we observe that both modified DLN and DLN-SAV algorithms have second-order accuracy in time for the 1D traveling wave problem, confirming the expected time-stepping accuracy of these algorithms. Next, we set $k = h^2$ to check the accuracy of both algorithms in space. From Tables 2 and 4, we can see that both algorithms demonstrate third-order spatial convergence for $\ell^\infty(L^2)$ -norm and second-order spatial convergence for $\ell^2(H^1)$ -norm.

Table 3 L^2 -norm of error and rate for 1D DLN-SAV scheme in time ($h = k^2$)

	k	$\ u - u^h\ _{\ell^\infty(L^2)}$	R	$\ u - u^h\ _{\ell^2(L^2)}$	R	$\ u - u^h\ _{\ell^2(H^1)}$	R
$\theta = \frac{2}{3}$	0.04	4.94e-5	-	3.82e-5	-	2.09e-3	-
	0.02	1.26e-5	1.98	9.64e-6	1.98	4.82e-4	2.12
	0.01	3.17e-6	1.99	2.42e-6	1.99	1.20e-4	2.00
	0.005	7.94e-7	1.99	6.07e-7	2.00	3.01e-5	2.00
$\theta = \frac{2}{\sqrt{5}}$	0.04	6.05e-5	-	4.61e-5	-	2.07e-3	-
	0.02	1.54e-5	1.97	1.17e-5	1.98	4.77e-4	2.11
	0.01	3.90e-6	1.99	2.94e-6	1.99	1.19e-4	2.00
	0.005	9.79e-7	1.99	7.38e-7	2.00	2.99e-5	2.00
$\theta = 1$	0.04	6.61e-5	-	5.03e-5	-	2.05e-3	-
	0.02	1.69e-5	1.97	1.28e-5	1.98	4.74e-4	2.11
	0.001	4.26e-6	1.99	3.21e-6	1.99	1.18e-4	2.00
	0.005	1.07e-6	1.99	8.06e-7	1.99	2.97e-5	2.00

Table 4 L^2 -norm of error and rate for 1D DLN-SAV scheme in space ($k = h^2$)

	h	$\ u - u^h\ _{\ell^\infty(L^2)}$	R	$\ u - u^h\ _{\ell^2(L^2)}$	R	$\ u - u^h\ _{\ell^2(H^1)}$	R
$\theta = \frac{2}{3}$	0.04	2.17e-3	-	2.41e-3	-	4.80e-1	-
	0.02	2.91e-4	2.90	3.97e-4	2.60	1.32e-1	1.86
	0.01	3.69e-5	2.98	5.19e-5	2.94	3.39e-2	1.97
	0.005	4.65e-6	2.99	6.57e-6	2.98	8.53e-3	1.99
$\theta = \frac{2}{\sqrt{5}}$	0.04	2.17e-3	-	2.41e-3	-	4.80e-1	-
	0.02	2.91e-4	2.90	3.97e-4	2.60	1.32e-1	1.86
	0.01	3.69e-5	2.98	5.19e-5	2.94	3.39e-2	1.97
	0.005	4.65e-6	2.99	6.57e-6	2.98	8.53e-3	1.99
$\theta = 1$	0.04	2.17e-3	-	2.41e-3	-	4.80e-1	-
	0.02	2.91e-4	2.90	3.97e-4	2.60	1.32e-1	1.86
	0.01	3.69e-5	2.98	5.19e-5	2.94	3.39e-2	1.97
	0.005	4.65e-6	2.99	6.57e-6	2.98	8.53e-3	1.99

6.1.2 Variable Time Step

We utilize constant time step k as a reference time step and set $h = k^2$ to test the accuracy of the variable time-stepping modified DLN algorithm (19) and DLN-SAV algorithm (53) over time. Two different time step scenarios are considered:

1. Randomized Time Steps: For each time step, we set $k_n = k + k \cdot rand$, where $rand$ is a random number drawn from the uniform distribution in the interval (0,1).
2. Alternating Time Steps: We alternate the time step size as follows: $k_1 = k, k_2 = 2k, k_3 = k, k_4 = 2k, \dots$

Table 5 L^2 -norm of error and rate for 1D modified DLN scheme in time ($k_n = k + k \cdot rand$; $h = k^2$)

	k	k_{max}	$\ u - u^h\ _{L^\infty(L^2)}$	R	$\ u - u^h\ _{L^2(L^2)}$	R	$\ u - u^h\ _{L^2(H^1)}$	R
$\theta = \frac{2}{3}$	0.1	0.1919	2.20e-4	-	2.06e-4	-	3.45e-2	-
	0.05	0.0991	5.98e-5	1.97	5.33e-5	2.04	3.45e-3	3.48
	0.04	0.0771	3.36e-5	2.31	3.02e-5	2.28	1.80e-3	2.61
	0.02	0.0399	1.01e-5	1.82	8.58e-6	1.91	4.50e-4	2.10
$\theta = \frac{2}{\sqrt{5}}$	0.1	0.1995	1.85e-4	-	1.48e-4	-	3.34e-2	-
	0.05	0.0992	5.61e-5	1.71	4.57e-5	1.68	2.71e-3	3.60
	0.04	0.0789	3.56e-5	1.99	2.72e-5	2.26	1.32e-3	3.13
	0.02	0.0398	8.16e-6	2.15	6.37e-6	2.12	2.37e-4	2.51
$\theta = 1$	0.1	0.1738	1.53e-4	-	1.30e-4	-	3.32e-2	-
	0.05	0.0994	4.81e-5	2.07	3.55e-5	2.32	2.40e-3	4.70
	0.04	0.0787	3.01e-5	2.00	2.28e-5	1.91	1.15e-3	3.22
	0.02	0.0391	7.86e-6	1.92	6.03e-6	1.90	2.02e-4	2.47

For both test scenarios, the time steps lie within the range $[k, 2k]$. The accuracy rate is calculated using the formula:

$$Rate = \frac{\ln(Error_1/Error_2)}{\ln(k_{max,1}/k_{max,2})}$$

where $Error_1$ and $Error_2$ are the errors corresponding to the maximum time steps $k_{max,1}$ and $k_{max,2}$, respectively.

From Tables 5 - 8, our observation indicates that both algorithms with all θ values achieve second-order accuracy in time for the 1D traveling wave problem, even under non-uniform time steps. This is better than the first order convergence in time that we can prove in Theorem 2 for the non-uniform time step case.

To further test the order of accuracy of the modified DLN scheme, we apply the modified DLN method on the corresponding ODE $dy/dt + f(y) = 0$, assuming $y = y(t)$ is only time-dependent. We have carried out extensive numerical investigation of this test with different ways to determine the non-uniform time step size and different choices of $f(u)$. All of these tests demonstrate a second-order convergence numerically.

6.1.3 Comparison of the modified DLN and DLN-CSS algorithms

In this subsection, we compare the modified DLN algorithm with the DLN-CSS algorithm in (21) in terms of accuracy and efficiency. Both algorithms are implicit and need certain non-linear solver at each time step. From Tables 9 and 10, both algorithms reach second-order accuracy in time and take about the same CPU time to complete simulation. However, the modified DLN algorithm is slightly more accurate than the DLN-CSS algorithm, possibly due to the fact that the modified DLN algorithm addresses the whole non-linear term implicitly.

6.1.4 Adaptive Algorithms

Next, we test the accuracy and efficiency of the adaptive DLN algorithm in Algorithm 1, by comparing it with the corresponding constant time step algorithms. For adaptive algorithms,

Table 6 L^2 -norm of error and rate for 1D modified DLN scheme in time ($k_n = k, 2k, k, 2k, \dots; h = k^2$)

	k	k_{max}	$\ u - u^h\ _{\ell^\infty(L^2)}$	R	$\ u - u^h\ _{\ell^2(L^2)}$	R	$\ u - u^h\ _{\ell^2(H^1)}$	R
$\theta = \frac{2}{3}$	0.1	0.2	2.32e-4	-	2.51e-4	-	3.56e-2	-
	0.05	0.1	6.20e-5	1.90	6.26e-5	2.00	4.04e-3	3.14
	0.04	0.08	3.89e-5	2.08	4.00e-5	2.01	2.37e-3	2.40
	0.02	0.04	1.01e-5	1.95	1.00e-5	1.99	5.60e-4	2.08
$\theta = \frac{2}{\sqrt{5}}$	0.1	0.2	2.28e-4	-	1.96e-4	-	3.37e-2	-
	0.05	0.1	5.97e-5	1.93	4.75e-5	2.05	2.76e-3	3.61
	0.04	0.08	3.79e-5	2.03	3.03e-5	2.01	1.43e-3	2.95
	0.02	0.04	9.71e-6	1.97	7.54e-6	2.01	2.86e-4	2.32
$\theta = 1$	0.1	0.2	2.28e-4	-	1.91e-4	-	3.34e-2	-
	0.05	0.1	5.95e-5	1.93	4.62e-5	2.05	2.57e-3	3.70
	0.04	0.08	3.80e-5	2.02	2.95e-5	2.02	1.28e-3	3.13
	0.02	0.04	9.70e-6	1.97	7.35e-6	2.00	2.41e-4	2.41

Table 7 L^2 -norm of error and rate for 1D DLN-SAV scheme in time ($k_n = k + k \cdot rand; h = k^2$)

	k	k_{max}	$\ u - u^h\ _{\ell^\infty(L^2)}$	R	$\ u - u^h\ _{\ell^2(L^2)}$	R	$\ u - u^h\ _{\ell^2(H^1)}$	R
$\theta = \frac{2}{3}$	0.1	0.1885	6.25e-4	-	4.85e-4	-	4.16e-2	-
	0.05	0.1000	1.62e-4	2.13	1.31e-4	2.07	6.75e-3	2.87
	0.04	0.0781	1.20e-4	1.20	9.35e-5	1.36	4.80e-3	1.37
	0.02	0.0399	3.10e-5	2.02	2.45e-5	1.99	1.22e-3	2.04
$\theta = \frac{2}{\sqrt{5}}$	0.1	0.1931	7.12e-4	-	5.64e-4	-	4.10e-2	-
	0.05	0.0987	2.20e-4	1.76	1.66e-4	1.82	7.20e-3	2.59
	0.04	0.0744	1.28e-4	1.89	9.68e-5	1.91	4.05e-3	2.03
	0.02	0.0400	3.74e-5	1.98	2.80e-5	2.00	1.15e-3	2.03
$\theta = 1$	0.1	0.1996	8.19e-4	-	6.41e-4	-	4.13e-2	-
	0.05	0.0998	2.58e-4	1.67	2.04e-4	1.65	7.94e-3	2.38
	0.04	0.0770	1.38e-4	2.42	1.05e-4	2.57	4.04e-3	2.62
	0.02	0.0396	3.86e-5	1.91	2.96e-5	1.90	1.11e-3	1.93

the following setup is adopted: the tolerance Tol = 1.e - 6, the minimum time step $k_{min} = 1.e - 5$, the maximum time step $k_{max} = 0.1$, two initial time steps $k_0 = k_1 = 1.e - 3$, and the safety factor $\kappa = 0.8$. For constant step algorithms, we set the constant time step as $k = 1.e - 3$. From Tables 11 and 12, we observe that both adaptive algorithms outperform the constant step algorithms. Adaptive algorithms take much fewer time steps to obtain the same accuracy for all three θ values, when compared with the corresponding constant step algorithms.

Table 8 L^2 -norm of error and rate for 1D DLN-SAV scheme in time ($k_n = k, 2k, k, 2k, \dots; h = k^2$)

	k	k_{\max}	$\ u - u^h\ _{\ell^\infty(L^2)}$	R	$\ u - u^h\ _{\ell^2(L^2)}$	R	$\ u - u^h\ _{\ell^2(H^1)}$	R
$\theta = \frac{2}{3}$	0.1	0.2	6.52e-4	-	5.53e-4	-	4.37e-2	-
	0.05	0.1	1.76e-4	1.89	1.41e-4	1.97	7.41e-3	2.56
	0.04	0.08	1.14e-4	1.96	9.07e-5	1.99	4.64e-3	2.10
	0.02	0.04	2.94e-5	1.95	2.29e-5	1.99	1.15e-3	2.01
$\theta = \frac{2}{\sqrt{5}}$	0.1	0.2	7.95e-4	-	6.57e-4	-	4.36e-2	-
	0.05	0.1	2.18e-4	1.86	1.71e-4	1.94	7.47e-3	2.55
	0.04	0.08	1.40e-4	1.97	1.10e-4	1.98	4.68e-3	2.09
	0.02	0.04	3.63e-5	1.95	2.78e-5	1.98	1.16e-3	2.01
$\theta = 1$	0.1	0.2	8.66e-4	-	7.10e-4	-	4.35e-2	-
	0.05	0.1	2.38e-4	1.86	1.86e-4	1.93	7.45e-3	2.54
	0.04	0.08	1.54e-4	1.97	1.20e-4	1.97	4.67e-3	2.09
	0.02	0.04	3.98e-5	1.95	3.04e-5	1.98	1.16e-3	2.01

Table 9 L^2 -norm and H^1 -norm of error and rate for 1D DLN-CSS scheme in time ($h = k^2$)

	k	$\ u - u^h\ _{\ell^\infty(L^2)}$	R	$\ u - u^h\ _{\ell^2(H^1)}$	R	CPU Time
$\theta = \frac{2}{3}$	0.04	5.78e-5	-	2.85e-3	-	69.89
	0.02	1.46e-5	1.98	6.89e-4	2.05	434.90
	0.01	3.68e-6	1.99	1.72e-4	2.00	3419.14
$\theta = \frac{2}{\sqrt{5}}$	0.04	6.77e-05	-	2.96e-03	-	55.88
	0.02	1.72e-05	1.98	7.12e-04	2.05	437.49
	0.01	4.33e-06	1.99	1.78e-04	2.00	3464.64
$\theta = 1$	0.04	7.25e-5	-	2.98e-3	-	56.17
	0.02	1.85e-5	1.98	7.20e-4	2.05	442.03
	0.01	4.65e-6	1.99	1.80e-4	2.00	3475.37

Table 10 L^2 -norm and H^1 -norm of error and rate for 1D modified DLN scheme in time ($h = k^2$)

	k	$\ u - u^h\ _{\ell^\infty(L^2)}$	R	$\ u - u^h\ _{\ell^2(H^1)}$	R	CPU Time
$\theta = \frac{2}{3}$	0.04	1.84e-5	-	1.05e-3	-	72.18
	0.02	4.64e-6	1.98	1.58e-4	2.73	431.92
	0.01	1.17e-6	1.99	3.74e-5	2.08	3494.29
$\theta = \frac{2}{\sqrt{5}}$	0.04	1.45e-5	-	9.38e-4	-	61.00
	0.02	3.68e-6	1.98	1.05e-4	3.16	452.98
	0.01	9.27e-7	1.99	2.27e-5	2.21	3506.87
$\theta = 1$	0.04	1.27e-5	-	9.19e-4	-	57.17
	0.02	3.22e-6	1.98	9.45e-5	3.28	443.27
	0.01	8.12e-7	1.99	1.97e-5	2.26	3519.10

Table 11 Errors and number of time steps of the adaptive and constant time-stepping 1D modified DLN schemes

Adaptive modified DLN schemes					
θ	$\ u - u^h\ _{\ell^\infty(L^2)}$	$\ u - u^h\ _{\ell^2(L^2)}$	$\ u - u^h\ _{\ell^2(H^1)}$	# Steps	# Rejections
$\theta = \frac{2}{3}$	3.69e-5	3.67e-5	2.39e-2	653	341
$\theta = \frac{2}{\sqrt{5}}$	3.69e-5	3.67e-5	2.39e-2	264	93
$\theta = 1$	3.69e-5	3.67e-5	2.39e-2	148	43
Constant time-stepping modified DLN schemes					
θ	$\ u - u^h\ _{\ell^\infty(L^2)}$	$\ u - u^h\ _{\ell^2(L^2)}$	$\ u - u^h\ _{\ell^2(H^1)}$	# Steps	# Rejections
$\theta = \frac{2}{3}$	3.69e-5	3.67e-5	2.39e-2	1000	-
$\theta = \frac{2}{\sqrt{5}}$	3.69e-5	3.67e-5	2.39e-2	1000	-
$\theta = 1$	3.69e-5	3.67e-5	2.39e-2	1000	-

Table 12 Errors and number of time steps of the adaptive and constant time-stepping 1D DLN-SAV schemes

Adaptive DLN-SAV schemes					
θ	$\ u - u^h\ _{\ell^\infty(L^2)}$	$\ u - u^h\ _{\ell^2(L^2)}$	$\ u - u^h\ _{\ell^2(H^1)}$	# Steps	# Rejections
$\theta = \frac{2}{3}$	3.68e-5	3.67e-5	2.39e-2	174	65
$\theta = \frac{2}{\sqrt{5}}$	3.67e-5	3.67e-5	2.39e-2	146	36
$\theta = 1$	3.67e-5	3.67e-5	2.39e-2	140	43
Constant time-stepping DLN-SAV schemes					
θ	$\ u - u^h\ _{\ell^\infty(L^2)}$	$\ u - u^h\ _{\ell^2(L^2)}$	$\ u - u^h\ _{\ell^2(H^1)}$	# Steps	# Rejections
$\theta = \frac{2}{3}$	3.68e-5	3.67e-5	2.39e-2	1000	-
$\theta = \frac{2}{\sqrt{5}}$	3.68e-5	3.67e-5	2.39e-2	1000	-
$\theta = 1$	3.68e-5	3.67e-5	2.39e-2	1000	-

6.2 Two-dimensional Example with Known Solution

We consider a two-dimensional example to verify that the proposed DLN algorithms are accurate and efficient for 2D test problems. As studied in [30], we consider the exact function of the form

$$u(x, y, t) = 0.05e^{-0.1t} \sin(x) \sin(y), \quad (x, y) \in [0, 2\pi] \times [0, 2\pi], \quad 0 \leq t \leq T, \quad (109)$$

with the homogeneous boundary condition. Since this function does not satisfy the Allen-Cahn equation (1) exactly, we add the extra source term

$$g(x, y, t) = 0.05(2\epsilon^2 - 1.1)e^{-0.1t} \sin(x) \sin(y) + (0.05e^{-0.1t} \sin(x) \sin(y))^3$$

such that $u(x, y, t)$ in (109) is the exact solution to the revised Allen-Cahn equation

$$u_t - \epsilon^2 \Delta u + f(u) = g(x, y, t).$$

with the model parameter $\epsilon = 0.01$. \mathbb{P}^2 finite element space is again used.

Table 13 L^2 -norm of error and rate for 2D modified DLN scheme in time ($N = 500$)

	k	$\ u - u^h\ _{\ell^\infty(L^2)}$	R	$\ u - u^h\ _{\ell^2(L^2)}$	R	$\ u - u^h\ _{\ell^2(H^1)}$	R
$\theta = \frac{2}{3}$	0.4	1.80e-3	-	1.51e-3	-	2.13e-3	-
	0.2	5.25e-4	1.78	4.03e-4	1.90	5.70e-4	1.90
	0.1	1.43e-4	1.88	1.05e-4	1.95	1.48e-4	1.95
	0.05	3.72e-5	1.94	2.66e-5	1.97	3.79e-5	1.97
$\theta = \frac{2}{\sqrt{5}}$	0.4	1.31e-3	-	1.10e-3	-	1.55e-3	-
	0.2	3.90e-4	1.75	3.00e-4	1.87	4.24e-4	1.87
	0.1	1.07e-4	1.86	7.87e-5	1.93	1.11e-4	1.93
	0.05	2.82e-5	1.93	2.02e-5	1.96	2.87e-5	1.95
$\theta = 1$	0.4	1.06e-3	-	8.84e-4	-	1.25e-3	-
	0.2	3.18e-4	1.73	2.44e-4	1.86	3.45e-4	1.86
	0.1	8.79e-5	1.85	6.44e-5	1.92	9.12e-5	1.92
	0.05	2.31e-5	1.93	1.65e-5	1.96	2.37e-5	1.94

Table 14 L^2 -norm of error and rate for 2D modified DLN scheme in space ($k = 0.01$)

	N	$\ u - u^h\ _{\ell^\infty(L^2)}$	R	$\ u - u^h\ _{\ell^2(L^2)}$	R	$\ u - u^h\ _{\ell^2(H^1)}$	R
$\theta = \frac{2}{3}$	20	4.98e-5	-	2.57e-5	-	1.48e-3	-
	40	6.08e-6	3.03	3.18e-6	3.02	3.78e-4	1.97
	60	1.51e-6	3.43	8.03e-7	3.39	1.59e-4	2.14
	80	5.74e-7	3.36	3.12e-7	3.29	8.81e-5	2.04
	100	2.65e-7	3.46	1.46e-7	3.39	5.48e-5	2.13
$\theta = \frac{2}{\sqrt{5}}$	20	4.97e-5	-	2.57e-5	-	1.48e-3	-
	40	6.07e-6	3.03	3.17e-6	3.02	3.78e-4	1.97
	60	1.51e-6	3.43	8.02e-7	3.39	1.59e-4	2.14
	80	5.73e-7	3.37	3.11e-7	3.29	8.81e-5	2.04
	100	2.63e-7	3.48	1.45e-7	3.41	5.47e-5	2.13
$\theta = 1$	20	4.96e-5	-	2.56e-5	-	1.48e-3	-
	40	6.06e-6	3.03	3.17e-6	3.02	3.78e-4	1.97
	60	1.51e-6	3.43	8.01e-7	3.39	1.59e-4	2.14
	80	5.72e-7	3.37	3.11e-7	3.29	8.81e-5	2.04
	100	2.63e-7	3.49	1.45e-7	3.42	5.47e-5	2.13

6.2.1 Constant Time Step

To confirm the time convergence rate, we first set the final time as $T = 4$ and consider a refined triangular mesh with $N = 500$ nodes on each side of the boundaries. Tables 13 and 15 show that both modified DLN and DLN-SAV algorithms achieved second-order convergence in time for the 2D test problem in (109). Then we set the final time $T = 1$ and the constant time step $k = 0.01$ to check the spatial convergence. We observe from Tables 14 and 16 that both algorithms have third-order accuracy in L^2 -norm and second-order accuracy in H^1 -norm.

Table 15 L^2 -norm of error and rate for 2D DLN-SAV scheme in time ($N = 500$)

	k	$\ u - u^h\ _{\ell^\infty(L^2)}$	R	$\ u - u^h\ _{\ell^2(L^2)}$	R	$\ u - u^h\ _{\ell^2(H^1)}$	R
$\theta = \frac{2}{3}$	0.4	1.47e-3	-	1.25e-3	-	1.77e-3	-
	0.2	5.08e-4	1.53	3.92e-4	1.67	5.55e-4	1.67
	0.1	1.45e-4	1.81	1.07e-4	1.88	1.51e-4	1.88
	0.05	3.84e-5	1.92	2.75e-5	1.96	3.91e-5	1.95
$\theta = \frac{2}{\sqrt{5}}$	0.4	2.07e-3	-	1.76e-3	-	2.49e-3	-
	0.2	7.39e-4	1.49	5.71e-4	1.63	8.07e-4	1.63
	0.1	2.15e-4	1.78	1.58e-4	1.86	2.23e-4	1.86
	0.05	5.72e-5	1.91	4.09e-5	1.94	5.80e-5	1.94
$\theta = 1$	0.4	2.36e-3	-	2.01e-3	-	2.84e-3	-
	0.2	8.53e-4	1.47	6.58e-4	1.61	9.31e-4	1.61
	0.1	2.49e-4	1.77	1.83e-4	1.85	2.59e-4	1.85
	0.05	6.67e-5	1.90	4.77e-5	1.94	6.76e-5	1.94

Table 16 L^2 -norm of error and rate for 2D DLN-SAV scheme in space ($k = 0.01$)

	N	$\ u - u^h\ _{\ell^\infty(L^2)}$	R	$\ u - u^h\ _{\ell^2(L^2)}$	R	$\ u - u^h\ _{\ell^2(H^1)}$	R
$\theta = \frac{2}{3}$	20	4.97e-5	-	2.57e-5	-	1.48e-3	-
	40	6.08e-6	3.03	3.18e-6	3.01	3.78e-4	1.97
	60	1.52e-6	3.43	8.07e-7	3.38	1.59e-4	2.14
	80	5.80e-7	3.34	3.15e-7	3.27	8.81e-5	2.04
	100	2.71e-7	3.41	1.49e-7	3.35	5.48e-5	2.13
$\theta = \frac{2}{\sqrt{5}}$	20	4.97e-5	-	2.56e-5	-	1.48e-3	-
	40	6.08e-6	3.03	3.18e-6	3.01	3.78e-4	1.97
	60	1.52e-6	3.42	8.06e-7	3.38	1.59e-4	2.14
	80	5.84e-7	3.32	3.16e-7	3.25	8.81e-5	2.04
	100	2.78e-7	3.32	1.53e-7	3.27	5.48e-5	2.13
$\theta = 1$	20	4.96e-5	-	2.56e-5	-	1.48e-3	-
	40	6.07e-6	3.03	3.17e-6	3.01	3.78e-4	1.97
	60	1.52e-6	3.42	8.06e-7	3.38	1.59e-4	2.14
	80	5.86e-7	3.31	3.17e-7	3.24	8.81e-5	2.04
	100	2.83e-7	3.26	1.55e-7	3.22	5.47e-5	2.13

6.2.2 Variable Time Step

Similar to Section 6.1.2, we test the accuracy of the variable time-stepping modified DLN algorithm (19) and DLN-SAV algorithm (53) over time for the 2D case, utilizing the randomized time step $k_n = k + k \cdot \text{rand}$. The final time is $T = 4.0$ and the number of nodes $N = 500$ on each side of the boundaries. The accuracy rate calculated using k_{\max} again demonstrates second-order temporal convergence rate numerically, as seen in Tables 17 and 18.

Table 17 L^2 -norm of error and rate for 2D modified DLN scheme in time ($k_n = k + k \cdot rand$; $N = 500$)

	k	k_{\max}	$\ u - u^h\ _{\ell^\infty(L^2)}$	R	$\ u - u^h\ _{\ell^2(L^2)}$	R	$\ u - u^h\ _{\ell^2(H^1)}$	R
$\theta = \frac{2}{3}$	0.4	0.7818	1.67e-2	-	1.59e-2	-	2.24e-2	-
	0.3	0.5851	8.64e-3	2.27	7.39e-3	2.63	1.05e-2	2.63
	0.2	0.3683	3.58e-3	1.90	2.94e-3	1.99	4.16e-3	1.99
	0.1	0.1987	9.36e-4	2.18	7.19e-4	2.28	1.02e-3	2.28
$\theta = \frac{2}{\sqrt{5}}$	0.4	0.7818	8.10e-3	-	7.69e-3	-	1.09e-2	-
	0.3	0.5851	4.26e-3	2.22	3.64e-3	2.58	5.15e-3	2.58
	0.2	0.3683	1.77e-3	1.89	1.45e-3	1.99	2.05e-3	1.99
	0.1	0.1987	4.71e-4	2.15	3.59e-4	2.26	5.08e-4	2.26
$\theta = 1$	0.4	0.7818	3.61e-3	-	3.41e-3	-	4.83e-3	-
	0.3	0.5851	1.93e-3	2.16	1.64e-3	2.54	2.32e-3	2.54
	0.2	0.3683	7.94e-4	1.92	6.46e-4	2.01	9.13e-4	2.01
	0.1	0.1987	2.14e-4	2.12	1.60e-4	2.26	2.27e-4	2.26

Table 18 L^2 -norm of error and rate for 2D DLN-SAV scheme in time ($k_n = k + k \cdot rand$; $N = 500$)

	k	k_{\max}	$\ u - u^h\ _{\ell^\infty(L^2)}$	R	$\ u - u^h\ _{\ell^2(L^2)}$	R	$\ u - u^h\ _{\ell^2(H^1)}$	R
$\theta = \frac{2}{3}$	0.4	0.7818	3.37e-3	-	3.27e-3	-	4.63e-3	-
	0.3	0.5851	2.17e-3	1.52	1.87e-3	1.94	2.64e-3	1.94
	0.2	0.3683	1.10e-3	1.47	9.02e-4	1.57	1.28e-3	1.57
	0.1	0.1987	3.10e-4	2.05	2.33e-4	2.20	3.29e-4	2.20
$\theta = \frac{2}{\sqrt{5}}$	0.4	0.7818	4.25e-3	-	4.12e-3	-	5.83e-3	-
	0.3	0.5851	2.87e-3	1.35	2.47e-3	1.76	3.50e-3	1.76
	0.2	0.3683	1.52e-3	1.38	1.25e-3	1.48	1.76e-3	1.48
	0.1	0.1987	4.48e-4	1.98	3.36e-4	2.13	4.75e-4	2.13
$\theta = 1$	0.4	0.7818	4.65e-3	-	4.51e-3	-	6.37e-3	-
	0.3	0.5851	3.21e-3	1.28	2.76e-3	1.69	3.90e-3	1.69
	0.2	0.3683	1.72e-3	1.35	1.41e-3	1.45	2.00e-3	1.45
	0.1	0.1987	5.16e-4	1.95	3.87e-4	2.10	5.47e-4	2.10

6.2.3 Adaptive Algorithms

Next, we compare Algorithm 1 and the corresponding constant time-stepping algorithms to show the accuracy and efficiency of time adaptivity. We set final time $T = 1$, model parameter $\epsilon = 0.01$, the number of nodes $N = 50$ on each side of the boundaries for both adaptive and constant algorithms. For adaptive algorithms, we set the maximum time step $k_{\max} = 0.1$, the minimum time step $k_{\min} = 1.e - 5$, two initial time step $k_0 = k_1 = 1.e - 3$, tolerance $Tol = 1.e - 8$ and safety factor $\kappa = 0.8$. We use time step $k = 1.e - 3$ for constant time-stepping algorithms. From Table 19, we can see that adaptive modified DLN algorithms, especially with $\theta = 2/3$ or 1, work more efficiently than the corresponding constant time-stepping algorithms, since the adaptive algorithms take much fewer number of time steps and obtain errors comparable to those of the constant step algorithms. For

Table 19 Errors and number of time steps of the adaptive and constant time-stepping 2D modified DLN schemes

Adaptive modified DLN schemes					
θ	$\ u - u^h\ _{\ell^\infty(L^2)}$	$\ u - u^h\ _{\ell^2(L^2)}$	$\ u - u^h\ _{\ell^2(H^1)}$	# Steps	# Rejections
$\theta = \frac{2}{3}$	3.02e-6	1.79e-6	2.37e-4	280	73
$\theta = \frac{2}{\sqrt{5}}$	4.86e-6	2.96e-6	2.38e-4	93	18
$\theta = 1$	2.96e-6	1.60e-6	2.37e-4	48	18
Constant time-stepping modified DLN schemes					
θ	$\ u - u^h\ _{\ell^\infty(L^2)}$	$\ u - u^h\ _{\ell^2(L^2)}$	$\ u - u^h\ _{\ell^2(H^1)}$	# Steps	# Rejections
$\theta = \frac{2}{3}$	2.97e-6	1.56e-6	2.37e-4	1000	-
$\theta = \frac{2}{\sqrt{5}}$	2.97e-6	1.56e-6	2.37e-4	1000	-
$\theta = 1$	2.97e-6	1.56e-6	2.37e-4	1000	-

Table 20 Errors and number of time steps of the adaptive and constant time-stepping 2D DLN-SAV schemes

Adaptive DLN-SAV schemes					
θ	$\ u - u^h\ _{\ell^\infty(L^2)}$	$\ u - u^h\ _{\ell^2(L^2)}$	$\ u - u^h\ _{\ell^2(H^1)}$	# Steps	# Rejections
$\theta = \frac{2}{3}$	3.03e-6	1.62e-6	2.37e-4	45	9
$\theta = \frac{2}{\sqrt{5}}$	3.08e-6	1.65e-6	2.37e-4	44	9
$\theta = 1$	3.11e-6	1.66e-6	2.37e-4	44	15
Constant time-stepping DLN-SAV schemes					
θ	$\ u - u^h\ _{\ell^\infty(L^2)}$	$\ u - u^h\ _{\ell^2(L^2)}$	$\ u - u^h\ _{\ell^2(H^1)}$	# Steps	# Rejections
$\theta = \frac{2}{3}$	2.97e-6	1.56e-6	2.37e-4	1000	-
$\theta = \frac{2}{\sqrt{5}}$	2.97e-6	1.56e-6	2.37e-4	1000	-
$\theta = 1$	2.97e-6	1.56e-6	2.37e-4	1000	-

DLN-SAV algorithms, we observe from Table 20 that adaptive algorithms have the same error magnitude as constant time-stepping algorithms. However, adaptive algorithms with all three θ values finish the simulation only in 45 time steps while the constant step algorithms take 1000 time steps.

6.3 Two-dimensional test with random initial value

In this example, we simulate 2D Allen-Cahn equation with random initial condition [21]:

$$u_0(x, y) = 0.1 \times \text{rand}(x, y) - 0.05, \quad (x, y) \in [0, 2\pi]^2,$$

where the function $\text{rand}(x, y)$ generates value uniformly distributed on $[0, 1]$ at point (x, y) . We set the model parameter ϵ to be 0.1 and number of nodes on each side of the boundaries to be 100 to generate a triangular mesh. We test the adaptive Algorithm 1 with periodic boundary condition.

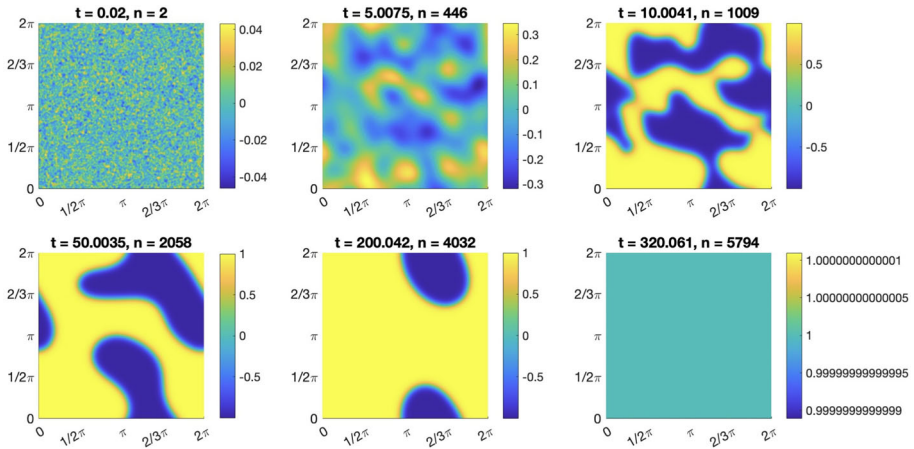


Fig. 1 2D Adaptive modified DLN algorithm with $\theta = 1$ converges to steady state with 5794 time steps

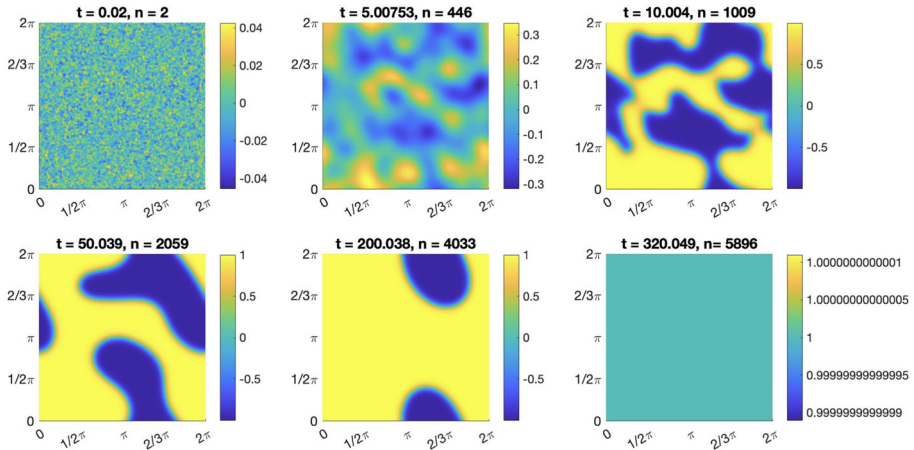


Fig. 2 2D Adaptive DLN-SAV algorithm with $\theta = 1$ converges to steady state with 5896 time steps

For both adaptive modified DLN and DLN-SAV algorithms, we set two initial time step $k_0 = k_1 = 0.01$, the maximum time step $k_{max} = 0.1$, the minimum step $k_{min} = 1.e - 5$, the tolerance for LTE Tol = $1.e - 6$, and safety factor $\kappa = 0.8$. We use the fixed point iteration with tolerance $1.e - 8$ for non-linear solver in the adaptive modified DLN algorithm. The results of three θ values ($2/3, 2/\sqrt{5}, 1$) are very close, thus we only present the numerical results for the case of $\theta = 1$. From Fig. 1 and Fig. 2, we observe that both modified DLN and DLN-SAV algorithms converge to the steady state at the time $T = 320$ with around 5800 time steps. We also test the corresponding constant time-stepping DLN algorithms with constant step $k = 0.01$ and observe that the constant time-stepping algorithms converge to the steady state with more than 30000 time steps. From this test problem, we demonstrate that the adaptive DLN algorithms are stable and possess superior time efficiency when compared to the corresponding constant time-stepping algorithms.

7 Conclusion

In this paper, we propose two time-efficient algorithms for the Allen-Cahn equation: the modified DLN scheme and the DLN-SAV scheme. We prove that the modified DLN scheme unconditionally satisfies the discrete energy dissipation law, and its numerical solutions under uniform time grids are second-order accurate in time. When $\theta = 1$, the scheme reduces to the modified midpoint rule, and its numerical solutions are second-order in time on arbitrary time grids. For the variable step DLN-SAV scheme, we show that the scheme approximately satisfies the discrete dissipation law. Moreover, its implementation can be simplified equivalently through a refactorization process on the BE-SAV algorithm. To further enhance the performance of both algorithms, we utilized a time-adaptive mechanism based on the LTE criterion.

We validate our methods through three main numerical tests. The 1D traveling wave test and the 2D test with an extra source term show that both algorithms are second-order accurate under arbitrary time step sizes. The 2D test with random initial conditions also verifies that the modified DLN scheme and the DLN-SAV scheme are long-time stable under non-uniform time grids. All three tests demonstrate that the time-adaptive versions of both algorithms outperform the corresponding constant step algorithms. These adaptive algorithms achieve the same level of accuracy while requiring significantly fewer time steps. The time-efficient DLN schemes can be easily applied to other complicated phase field model such as the Cahn-Hilliard equation or Cahn-Hilliard-Navier-Stokes model, Which will be left as our future endeavors.

Appendices

A Proof of Lemma 2

For any $\theta \in [0, 1)$, applying fundamental theorem of Calculus leads to

$$\begin{aligned} u_{n+1,\theta}(x) - u_{n,\theta}(x) &= \frac{1+\theta}{2}(u_{n+1}(x) - u_n(x)) + \frac{1-\theta}{2}(u_n(x) - u_{n-1}(x)) \\ &= \frac{1+\theta}{2} \int_{t_n}^{t_{n+1}} u_t(x, t) dt + \frac{1-\theta}{2} \int_{t_{n-1}}^{t_n} u_t(x, t) dt. \end{aligned}$$

By Hölder's inequality, we have

$$\begin{aligned} \|(u_{n+1,\theta} - u_{n,\theta})^2\|^2 &\leq \left(\frac{1+\theta}{2}\right)^4 \int_{\Omega} \left(\int_{t_{n-1}}^{t_{n+1}} |u_t(x, t)| dt\right)^4 dx \\ &\leq C(\theta) \int_{\Omega} \left(\int_{t_{n-1}}^{t_{n+1}} 1 dt\right)^3 \left(\int_{t_{n-1}}^{t_{n+1}} |u_t(x, t)|^4 dt\right) dx, \end{aligned}$$

which implies (10). Similarly,

$$\begin{aligned} \frac{u_{n+1,\theta} + u_{n,\theta}}{2} - u(t_n, \beta) &= \frac{u_{n+1,\theta} + u_{n,\theta}}{2} - u(t_n) + u(t_n) - u(t_n, \beta) \\ &= \frac{1+\theta}{4} \int_{t_n}^{t_{n+1}} u_t(x, t) dt - \frac{1-\theta}{4} \int_{t_{n-1}}^{t_n} u_t(x, t) dt - \int_{t_n}^{t_{n,\beta}} u_t(x, t) dt. \end{aligned}$$

Then Eq. (11) follows by the fact $t_{n,\beta} \in [t_{n-1}, t_{n+1}]$ and using Hölder’s inequality:

$$\begin{aligned} \left\| \frac{u_{n+1,\theta} + u_{n,\theta}}{2} - u(t_{n,\beta}) \right\|^2 &\leq \left(\frac{1 + \theta}{4} \right)^2 \int_{\Omega} \left(\int_{t_{n-1}}^{t_{n+1}} |u_t(x, t)| dt \right)^2 dx \\ &\leq C(\theta) \int_{\Omega} \left(\int_{t_{n-1}}^{t_{n+1}} 1 dt \right) \left(\int_{t_{n-1}}^{t_{n+1}} |u_t(x, t)|^2 dt \right) dx. \end{aligned}$$

For the case of $\theta = 1$, the corresponding conclusions for the midpoint rule are easy to verify and the details are omitted here.

Next, we consider the case of uniform time grids with constant time step k and aim to prove (14). Applying Taylor’s theorem with integral remainder

$$\begin{aligned} u(x, t_{n+1}) &= u(x, t_n) + u_t(x, t_n)k + \int_{t_n}^{t_{n+1}} u_{tt}(x, t)(t_{n+1} - t)dt, \\ u(x, t_{n-1}) &= u(x, t_n) - u_t(x, t_n)k + \int_{t_n}^{t_{n-1}} u_{tt}(x, t)(t_{n-1} - t)dt, \\ u(x, t_{n,\beta}) &= u(x, t_n) + u_t(x, t_n)(t_{n,\beta} - t_n) + \int_{t_n}^{t_{n,\beta}} u_{tt}(x, t)(t_{n,\beta} - t)dt \\ &= u(x, t_n) + u_t(x, t_n)(\beta_2^{(n)} - \beta_0^{(n)})k + \int_{t_n}^{t_{n,\beta}} u_{tt}(x, t)(t_{n,\beta} - t)dt, \end{aligned} \tag{110}$$

with (under uniform time grids)

$$\beta_2^{(n)} = \frac{1}{4}(2 + \theta - \theta^2), \quad \beta_0^{(n)} = \frac{1}{4}(2 - \theta - \theta^2),$$

gives

$$\begin{aligned} &\frac{u_{n+1,\theta} + u_{n,\theta}}{2} - u(x, t_{n,\beta}) \\ &= \frac{1 + \theta}{4}u(x, t_{n+1}) + \frac{1}{2}u(x, t_n) + \frac{1 - \theta}{4}u(x, t_{n-1}) - u(x, t_{n,\beta}) \\ &= \frac{1 + \theta}{4} \int_{t_n}^{t_{n+1}} u_{tt}(x, t)(t_{n+1} - t)dt + \frac{1 - \theta}{4} \int_{t_n}^{t_{n-1}} u_{tt}(x, t)(t_{n-1} - t)dt \\ &\quad - \int_{t_n}^{t_{n,\beta}} u_{tt}(x, t)(t_{n,\beta} - t)dt. \end{aligned}$$

Therefore, Eq. (14) follows from

$$\begin{aligned} &\left\| \frac{u_{n+1,\theta} + u_{n,\theta}}{2} - u(t_{n,\beta}) \right\|^2 \\ &\leq C(\theta) \int_{\Omega} \left(\int_{t_n}^{t_{n+1}} |u_{tt}(x, t)|^2 dt \int_{t_n}^{t_{n+1}} (t_{n+1} - t)^2 dt + \int_{t_{n-1}}^{t_n} |u_{tt}(x, t)|^2 dt \int_{t_{n-1}}^{t_n} (t - t_{n-1})^2 dt \right. \\ &\quad \left. + \int_{t_n}^{t_{n,\beta}} |u_{tt}(x, t)|^2 dt \int_{t_n}^{t_{n,\beta}} (t_{n,\beta} - t)^2 dt \right) dx \\ &\leq C(\theta)k^3 \int_{\Omega} \int_{t_{n-1}}^{t_{n+1}} |u_{tt}(x, t)|^2 dt dx. \end{aligned}$$

B Proof of Lemma 3

As in the proof of Lemma 2, we only prove the case $\theta \in [0, 1)$ below. The case for $\theta = 1$ can be shown easily following the same procedure. Also, it suffices to consider the case $r = 0$ below. Combining Taylor’s theorem with integral remainder (110) (but with variable time step sizes k_n and k_{n-1}) with the fact that $\beta_2^{(n)} + \beta_1^{(n)} + \beta_0^{(n)} = 1$ leads to

$$\begin{aligned}
 & u_{n,\beta}(x) - u(x, t_{n,\beta}) \\
 &= \beta_2^{(n)} \int_{t_n}^{t_{n+1}} u_{tt}(x, t)(t_{n+1} - t)dt + \beta_0^{(n)} \int_{t_n}^{t_{n-1}} u_{tt}(x, t)(t_{n-1} - t)dt \\
 &\quad - \int_{t_n}^{t_{n,\beta}} u_{tt}(x, t)(t_{n,\beta} - t)dt.
 \end{aligned} \tag{111}$$

Utilizing the Hölder’s inequality, and bounding $\beta_\ell^{(n)}$ by $C(\theta)$, we have

$$\begin{aligned}
 & \|u_{n,\beta}(\cdot) - u(\cdot, t_{n,\beta})\|^2 \\
 &\leq C(\theta) \int_{\Omega} \left[\int_{t_n}^{t_{n+1}} |u_{tt}(x, t)|(t_{n+1} - t)dt + \int_{t_{n-1}}^{t_n} |u_{tt}(x, t)|(t - t_{n-1})dt \right. \\
 &\quad \left. + \int_{t_n}^{t_{n,\beta}} |u_{tt}(x, t)||t_{n,\beta} - t|dt \right]^2 dx \\
 &\leq C(\theta) \int_{\Omega} \left[\left[\int_{t_n}^{t_{n+1}} |u_{tt}(x, t)|^2 dt \int_{t_n}^{t_{n+1}} (t_{n+1} - t)^2 dt \right]^{\frac{1}{2}} + \left[\int_{t_{n-1}}^{t_n} |u_{tt}(x, t)|^2 dt \int_{t_{n-1}}^{t_n} (t - t_{n-1})^2 dt \right]^{\frac{1}{2}} \right. \\
 &\quad \left. + \left[\int_{t_n}^{t_{n,\beta}} |u_{tt}(x, t)|^2 dt \int_{t_n}^{t_{n,\beta}} (t_{n,\beta} - t)^2 dt \right]^{\frac{1}{2}} \right]^2 dx \\
 &\leq C(\theta)(k_n + k_{n-1})^3 \int_{\Omega} \int_{t_{n-1}}^{t_{n+1}} |u_{tt}(x, t)|^2 dt dx,
 \end{aligned}$$

which implies (15) with $r = 0$.

Next, we consider Eq. (16). We again consider Taylor’s theorem with integral remainder

$$\begin{aligned}
 u(x, t_{n+1}) &= u(x, t_n) + u_t(x, t_n)k_n + u_{tt}(x, t_n)\frac{k_n^2}{2} + \int_{t_n}^{t_{n+1}} u_{ttt}(x, t)\frac{(t_{n+1} - t)^2}{2} dt, \\
 u(x, t_{n-1}) &= u(x, t_n) - u_t(x, t_n)k_{n-1} + u_{tt}(x, t_n)\frac{k_{n-1}^2}{2} + \int_{t_n}^{t_{n-1}} u_{ttt}(x, t)\frac{(t_{n-1} - t)^2}{2} dt, \\
 u_t(x, t_{n,\beta}) &= u_t(x, t_n) + u_{tt}(x, t_n)(\beta_2^{(n)}k_n - \beta_0^{(n)}k_{n-1}) + \int_{t_n}^{t_{n,\beta}} u_{ttt}(x, t)(t_{n,\beta} - t)dt.
 \end{aligned}$$

and combine them with the fact that $\alpha_2 + \alpha_1 + \alpha_0 = 0$ to obtain

$$\begin{aligned}
 & \frac{u_{n,\alpha}(x)}{\widehat{k}_n} - u_t(t_{n,\beta}) \\
 &= \left[\frac{\alpha_2 k_n^2 + \alpha_0 k_{n-1}^2}{2\widehat{k}_n} - (\beta_2^{(n)}k_n - \beta_0^{(n)}k_{n-1}) \right] u_{tt}(x, t_n) - \int_{t_n}^{t_{n,\beta}} u_{ttt}(x, t)(t_{n,\beta} - t)dt \\
 &\quad + \frac{\alpha_2}{\widehat{k}_n} \int_{t_n}^{t_{n+1}} u_{ttt}(x, t)(t_{n+1} - t)^2 dt + \frac{\alpha_0}{\widehat{k}_n} \int_{t_n}^{t_{n-1}} u_{ttt}(x, t)(t_{n-1} - t)^2 dt.
 \end{aligned}$$

It's easy to check

$$\frac{\alpha_2 k_n^2 + \alpha_0 k_{n-1}^2}{2\widehat{k}_n} - (\beta_2^{(n)} k_n - \beta_0^{(n)} k_{n-1}) = 0. \tag{112}$$

Therefore,

$$\begin{aligned} & \left\| \frac{u_{n,\alpha}(\cdot)}{\widehat{k}_n} - u_t(x, t_n, \beta) \right\|^2 \\ & \leq \frac{C(\theta)}{\widehat{k}_n^2} \int_{\Omega} \left[\int_{t_n}^{t_{n+1}} |u_{ttt}(x, t)|(t_{n+1} - t)^2 dt + \int_{t_{n-1}}^{t_n} |u_{ttt}(x, t)|(t_{n-1} - t)^2 dt \right. \\ & \quad \left. + \widehat{k}_n \int_{t_n}^{t_{n,\beta}} |u_{ttt}(x, t)||t_{n,\beta} - t| dt \right]^2 dx \\ & \leq \frac{C(\theta)}{\widehat{k}_n^2} \int_{\Omega} \left\{ \left[\int_{t_n}^{t_{n+1}} |u_{ttt}(x, t)|^2 dt \int_{t_n}^{t_{n+1}} (t_{n+1} - t)^4 dt \right]^{\frac{1}{2}} + \left[\int_{t_{n-1}}^{t_n} |u_{ttt}(x, t)|^2 dt \int_{t_{n-1}}^{t_n} (t - t_{n-1})^4 dt \right]^{\frac{1}{2}} \right. \\ & \quad \left. + \widehat{k}_n \left[\int_{t_n}^{t_{n,\beta}} |u_{ttt}(x, t)|^2 dt \int_{t_n}^{t_{n,\beta}} (t_{n,\beta} - t)^2 dt \right]^{\frac{1}{2}} \right\}^2 dx \\ & \leq C(\theta) \frac{(k_n + k_{n-1})^2 + \widehat{k}_n^2}{\widehat{k}_n^2} (k_n + k_{n-1})^3 \int_{\Omega} \int_{t_{n-1}}^{t_{n+1}} |u_{ttt}(x, t)|^2 dt dx \\ & \leq C(\theta) (k_n + k_{n-1})^3 \int_{\Omega} \int_{t_{n-1}}^{t_{n+1}} |u_{ttt}(x, t)|^2 dt dx, \end{aligned}$$

where the last inequality follows from $\widehat{k}_n = \frac{1+\theta}{2} k_n + \frac{1-\theta}{2} k_{n-1}$. The case with $r \geq 0$ can be proven in the same way.

Acknowledgements This work was initiated during D. Luo's participation in the 2023 Research Opportunities in Mathematics for Underrepresented Students (ROMUS) program at the Ohio State University (OSU) Department of Mathematics. The authors gratefully acknowledge the support provided by OSU and the NSF grant DMS-1753581.

Author Contributions The first two authors Y. Chen and D. Luo contributed equally to this work.

Funding Y. Xing is partially supported by the National Science Foundation (NSF) grants DMS-1753581 and DMS-2309590.

Data Availability The code and datasets of this work are available from the corresponding author upon reasonable request.

Declarations

Ethical Approval The authors agree that this manuscript has followed the rules of ethics presented in the journal's Ethical Guidelines for Journal Publication.

Conflicts of Interest The authors have no relevant financial or non-financial interests to disclose.

Open Access This article is licensed under a Creative Commons Attribution 4.0 International License, which permits use, sharing, adaptation, distribution and reproduction in any medium or format, as long as you give appropriate credit to the original author(s) and the source, provide a link to the Creative Commons licence, and indicate if changes were made. The images or other third party material in this article are included in the article's Creative Commons licence, unless indicated otherwise in a credit line to the material. If material is not included in the article's Creative Commons licence and your intended use is not permitted by statutory

regulation or exceeds the permitted use, you will need to obtain permission directly from the copyright holder. To view a copy of this licence, visit <http://creativecommons.org/licenses/by/4.0/>.

References

1. Akrivis, G., Li, B., Li, D.: Energy-decaying extrapolated RK-SAV methods for the Allen-Cahn and Cahn-Hilliard equations. *SIAM J. Sci. Comput.* **41**(6), A3703–A3727 (2019)
2. Allen, S.M., Cahn, J.W.: A microscopic theory for antiphase boundary motion and its application to antiphase domain coarsening. *Acta Metallurgica* **27**(6), 1085–1095 (1979)
3. Bartels, S., Müller, R.: Error control for the approximation of Allen-Cahn and Cahn-Hilliard equations with a logarithmic potential. *Numer. Math.* **119**(3), 409–435 (2011)
4. Cheng, Q., Shen, J.: Multiple scalar auxiliary variable (MSAV) approach and its application to the phase-field vesicle membrane model. *SIAM J. Sci. Comput.* **40**(6), A3982–A4006 (2018)
5. Choi, J.-W., Lee, H.G., Jeong, D., Kim, J.: An unconditionally gradient stable numerical method for solving the Allen-Cahn equation. *Physica A: Statistical Mechanics and its Applications* **388**(9), 1791–1803 (2009)
6. Ciarlet, P. G.: The finite element method for elliptic problems, volume 40 of *Classics in Applied Mathematics*. Society for Industrial and Applied Mathematics (SIAM), Philadelphia, PA (2002). Reprint of the 1978 original [North-Holland, Amsterdam; MR0520174 (58 #25001)]
7. Condatte, N., Melcher, C., Süli, E.: Spectral approximation of pattern-forming nonlinear evolution equations with double-well potentials of quadratic growth. *Math. Comp.* **80**(273), 205–223 (2011)
8. Dahlquist, G. G.: On the relation of G-stability to other stability concepts for linear multistep methods. Dept. of Comp. Sci. Roy. Inst. of Technology, Report TRITA-NA-7621 (1976)
9. Dahlquist, G.G.: G-stability is equivalent to A-stability. *BIT* **18**(4), 384–401 (1978)
10. Dahlquist, G. G.: Positive functions and some applications to stability questions for numerical methods. In *Recent advances in numerical analysis* (Proc. Sympos., Math. Res. Center, Univ. Wisconsin, Madison, Wis., 1978), volume 41 of *Publ. Math. Res. Center Univ. Wisconsin*, pages 1–29. Academic Press, New York-London (1978)
11. Dahlquist, G.G., Liniger, W., Nevanlinna, O.: Stability of two-step methods for variable integration steps. *SIAM J. Numer. Anal.* **20**(5), 1071–1085 (1983)
12. Du, Q., Feng, X.: The phase field method for geometric moving interfaces and their numerical approximations. In *Geometric Partial Differential Equations - Part I*, volume 21 of *Handbook of Numerical Analysis*, pages 425–508. Elsevier (2020)
13. Du, Q., Nicolaides, R.A.: Numerical analysis of a continuum model of phase transition. *SIAM J. Numer. Anal.* **28**(5), 1310–1322 (1991)
14. Du, Q., Zhu, W.: Analysis and applications of the exponential time differencing schemes and their contour integration modifications. *BIT* **45**(2), 307–328 (2005)
15. Eyre, D. J.: Unconditionally gradient stable time marching the Cahn-Hilliard equation. In *Computational and mathematical models of microstructural evolution* (San Francisco, CA, 1998), volume 529 of *Math. Res. Soc. Sympos. Proc.*, pages 39–46. MRS, Warrendale, PA (1998)
16. Feng, X., Li, Y.: Analysis of symmetric interior penalty discontinuous Galerkin methods for the Allen-Cahn equation and the mean curvature flow. *IMA J. Numer. Anal.* **35**(4), 1622–1651 (2015)
17. Feng, X., Li, Y., Xing, Y.: Analysis of mixed interior penalty discontinuous Galerkin methods for the Cahn-Hilliard equation and the Hele-Shaw flow. *SIAM J. Numer. Anal.* **54**(2), 825–847 (2016)
18. Guan, Z., Lowengrub, J.S., Wang, C., Wise, S.M.: Second order convex splitting schemes for periodic nonlocal Cahn-Hilliard and Allen-Cahn equations. *J. Comput. Phys.* **277**, 48–71 (2014)
19. Guillén-González, F., Tierra, G.: On linear schemes for a Cahn-Hilliard diffuse interface model. *J. Comput. Phys.* **234**, 140–171 (2013)
20. Hairer, E., Nørsett, S., Wanner, G.: *Solving Ordinary Differential Equations II: Stiff and Differential-Algebraic Problems*. Springer, *Solving Ordinary Differential Equations* (1993)
21. He, D., Pan, K.: Maximum norm error analysis of an unconditionally stable semi-implicit scheme for multi-dimensional Allen-Cahn equations. *Numer. Methods Partial Differential Equations* **35**(3), 955–975 (2019)
22. Hecht, F.: New development in freefem++. *J. Numer. Math.* **20**(3–4), 251–265 (2012)
23. Heywood, J. G., Rannacher, R.: Finite-element approximation of the nonstationary Navier-Stokes problem. IV. Error analysis for second-order time discretization. *SIAM J. Numer. Anal.*, **27**(2):353–384 (1990)
24. Jeong, D., Kim, J.: An explicit hybrid finite difference scheme for the Allen-Cahn equation. *J. Comput. Appl. Math.* **340**, 247–255 (2018)

25. Ju, L., Zhang, J., Du, Q.: Fast and accurate algorithms for simulating coarsening dynamics of Cahn-Hilliard equations. *Computational Materials Science* **108**, 272–282 (2015)
26. Kulikov, G.Y., Shindin, S.K.: One-leg integration of ordinary differential equations with global error control. *Computational Methods in Applied Mathematics* **5**(1), 86–96 (2005)
27. Layton, W., Pei, W., Qin, Y., Trenchea, C.: Analysis of the variable step method of Dahlquist, Liniger and Nevanlinna for fluid flow. *Numer. Methods Partial Differential Equations* **38**(6), 1713–1737 (2022)
28. Layton, W., Pei, W., Trenchea, C.: Refactorization of a variable step, unconditionally stable method of Dahlquist, Liniger and Nevanlinna. *Appl. Math. Lett.*, 125:Paper No. 107789, 7 (2022)
29. Layton, W., Pei, W., Trenchea, C.: Time step adaptivity in the method of Dahlquist, Liniger and Nevanlinna. *Advances in Computational Science and Engineering* **1**(3), 320–350 (2023)
30. Li, C., Huang, Y., Yi, N.: An unconditionally energy stable second order finite element method for solving the Allen-Cahn equation. *J. Comput. Appl. Math.* **353**, 38–48 (2019)
31. Li, D., Qiao, Z.: On second order semi-implicit Fourier spectral methods for 2D Cahn-Hilliard equations. *J. Sci. Comput.* **70**(1), 301–341 (2017)
32. Li, H., Wang, D., Song, Z., Zhang, F.: Numerical analysis of an unconditionally energy-stable reduced-order finite element method for the Allen-Cahn phase field model. *Comput. Math. Appl.* **96**, 67–76 (2021)
33. Liao, H.-L., Tang, T., Zhou, T.: On energy stable, maximum-principle preserving, second-order BDF scheme with variable steps for the Allen-Cahn equation. *SIAM J. Numer. Anal.* **58**(4), 2294–2314 (2020)
34. Pan, Q., Chen, C., Zhang, Y. J., Yang, X.: A novel hybrid IGA-EIEQ numerical method for the Allen-Cahn/Cahn-Hilliard equations on complex curved surfaces. *Comput. Methods Appl. Mech. Engrg.*, 404:Paper No. 115767, 21 (2023)
35. Pei, W.: The semi-implicit DLN algorithm for the Navier-Stokes equations. *Numerical Algorithms* (2024)
36. Qin, Y., Chen, L., Wang, Y., Li, Y., Li, J.: An adaptive time-stepping DLN decoupled algorithm for the coupled Stokes-Darcy model. *Appl. Numer. Math.* **188**, 106–128 (2023)
37. Qin, Y., Hou, Y., Pei, W., Li, J.: A variable time-stepping algorithm for the unsteady Stokes/Darcy model. *J. Comput. Appl. Math.*, 394:Paper No. 113521, 14 (2021)
38. Shen, J., Wang, C., Wang, X., Wise, S.M.: Second-order convex splitting schemes for gradient flows with Ehrlich-Schwoebel type energy: application to thin film epitaxy. *SIAM J. Numer. Anal.* **50**(1), 105–125 (2012)
39. Shen, J., Xu, J.: Convergence and error analysis for the scalar auxiliary variable (SAV) schemes to gradient flows. *SIAM J. Numer. Anal.* **56**(5), 2895–2912 (2018)
40. Shen, J., Xu, J., Yang, J.: The scalar auxiliary variable (SAV) approach for gradient flows. *J. Comput. Phys.* **353**, 407–416 (2018)
41. Shen, J., Xu, J., Yang, J.: A new class of efficient and robust energy stable schemes for gradient flows. *SIAM Rev.* **61**(3), 474–506 (2019)
42. Shen, J., Yang, X.: Numerical approximations of Allen-Cahn and Cahn-Hilliard equations. *Discrete Contin. Dyn. Syst.* **28**(4), 1669–1691 (2010)
43. Shin, J., Lee, H.G., Lee, J.-Y.: Unconditionally stable methods for gradient flow using convex splitting Runge-Kutta scheme. *J. Comput. Phys.* **347**, 367–381 (2017)
44. Siddiqua, F., Pei, W.: Variable time step method of Dahlquist, Liniger and Nevanlinna (DLN) for a corrected Smagorinsky model. *arXiv preprint arXiv:2309.01867* (2023)
45. Song, H., Shu, C.-W.: Unconditional energy stability analysis of a second order implicit-explicit local discontinuous Galerkin method for the Cahn-Hilliard equation. *J. Sci. Comput.* **73**(2–3), 1178–1203 (2017)
46. Thomée, V.: Galerkin finite element methods for parabolic problems, volume 25 of Springer Series in Computational Mathematics. Springer-Verlag, Berlin, second edition (2006)
47. Wise, S.M., Wang, C., Lowengrub, J.S.: An energy-stable and convergent finite-difference scheme for the phase field crystal equation. *SIAM Journal on Numerical Analysis* **47**(3), 2269–2288 (2009)
48. Xu, J., Li, Y., Wu, S., Bousquet, A.: On the stability and accuracy of partially and fully implicit schemes for phase field modeling. *Comput. Methods Appl. Mech. Engrg.* **345**, 826–853 (2019)
49. Yan, Y., Chen, W., Wang, C., Wise, S.M.: A second-order energy stable BDF numerical scheme for the Cahn-Hilliard equation. *Commun. Comput. Phys.* **23**(2), 572–602 (2018)
50. Yang, X.: Error analysis of stabilized semi-implicit method of Allen-Cahn equation. *Discrete Contin. Dyn. Syst. Ser. B* **11**(4), 1057–1070 (2009)
51. Yang, X.: Efficient linear, stabilized, second-order time marching schemes for an anisotropic phase field dendritic crystal growth model. *Comput. Methods Appl. Mech. Engrg.* **347**, 316–339 (2019)

52. Yang, X., Ju, L.: Linear and unconditionally energy stable schemes for the binary fluid-surfactant phase field model. *Comput. Methods Appl. Mech. Engrg.* **318**, 1005–1029 (2017)
53. Zheng, N., Li, X.: New efficient and unconditionally energy stable schemes for the Cahn-Hilliard-Brinkman system. *Appl. Math. Lett.* **128**, 107918 (2022)

Publisher's Note Springer Nature remains neutral with regard to jurisdictional claims in published maps and institutional affiliations.